Precision Crystal Calorimeters in High Energy Physics: Past, Present and Future

Ren-Yuan Zhu

California Institute of Technology

Physics with Crystal Calorimeters

Charmonium system observed by CB through Inclusive photons

H→γγ at LHC

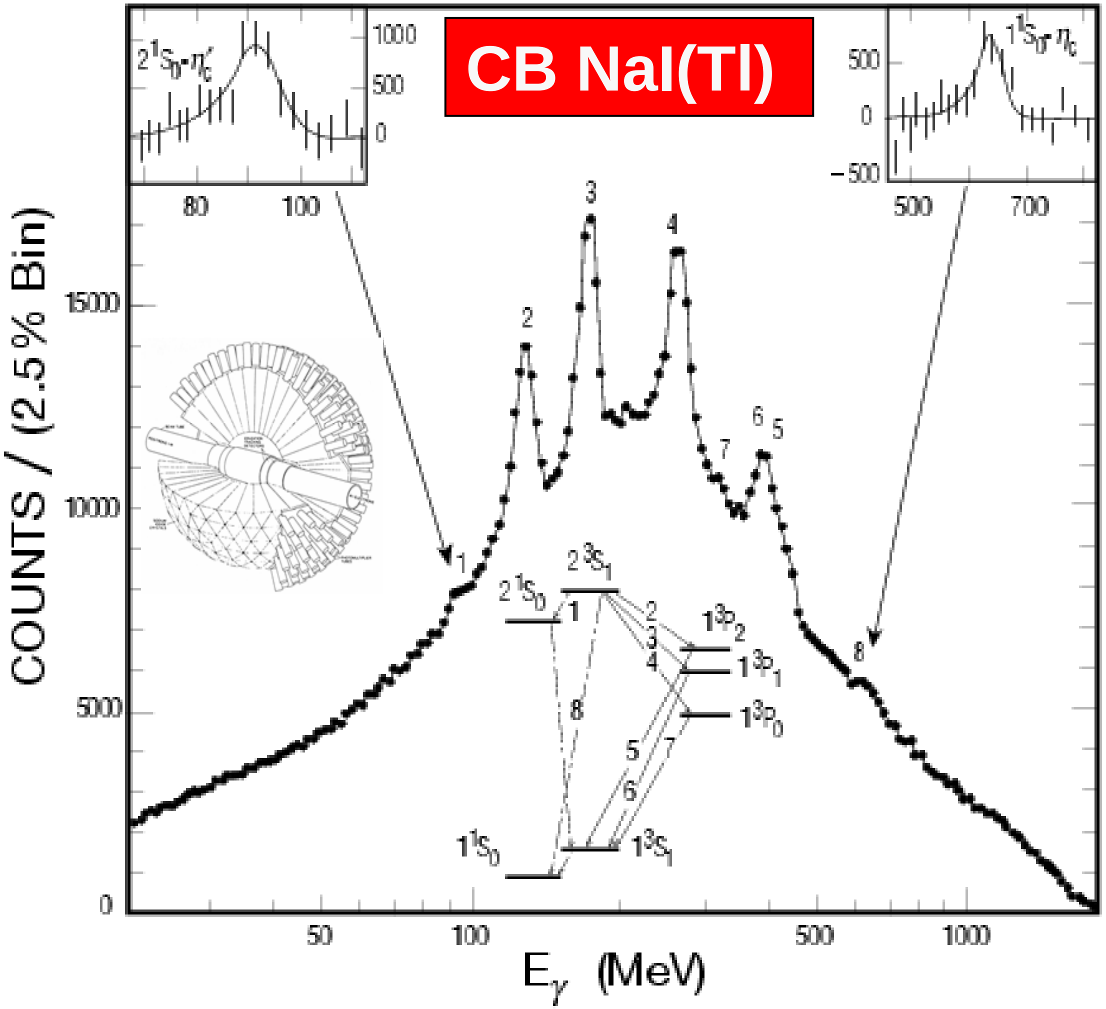

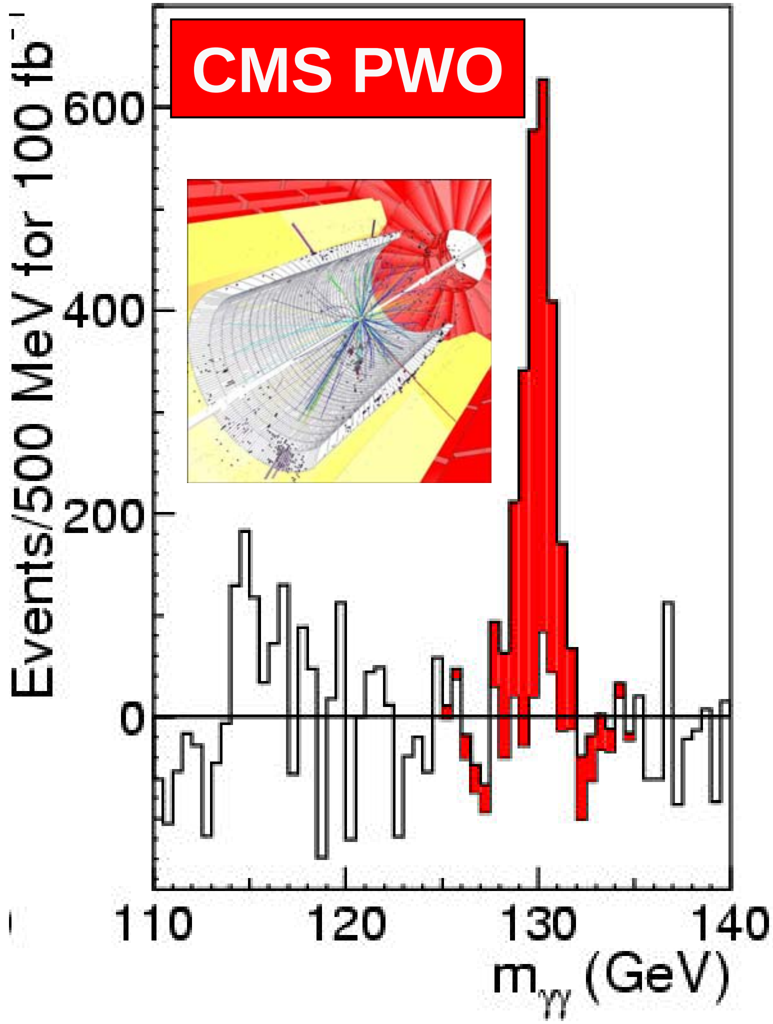

Mass Produced Crystals

Crystal	NaI(Tl)	CsI(Tl)	CsI	BaF_2	BGO	PWO(Y)	LSO(Ce)	GSO(Ce)
Density (g/cm^3)	3.67	4.51	4.51	4.89	7.13	8.3	7.40	6.71
Melting Point (ºC)	651	621	621	1280	1050	1123	2050	1950
Radiation Length (cm)	2.59	1.86	1.86	2.03	1.12	0.89	1.14	1.38
Molière Radius (cm)	4.13	3.57	3.57	3.10	2.23	2.00	2.07	2.23
Interaction Length (cm)	42.9	39.3	39.3	30.7	22.8	20.7	20.9	22.2
Refractive Index [a]	1.85	1.79	1.95	1.50	2.15	2.20	1.82	1.85
Hygroscopicity	Yes	Slight	Slight	No	No	No	No	No
Luminescence [b] (nm) (at peak)	410	550	420 310	300 220	480	425 420	402	440
Decay Time [b] (ns)	230	1250	30 6	630 0.9	300	30 6	40	60
Light Yield [b,c] (%)	100	165	3.6 1.1	36 3.4	21	0.29 .083	83	30
d(LY)/dT [b] (%/ ºC)	~0	0.3	-0.6	-2 ~0	-1.6	-1.9	~0	-0.1
Experiment	Crystal Ball	CLEO BaBar BELLE BES III	KTeV	TAPS (L*) (GEM)	L3 BELLE PANDA?	CMS ALICE PrimEx PANDA?	-	-

a. at peak of emission; b. up/low row: slow/fast component; c. PMT QE taken out.

Crystal Density: Radiation Length

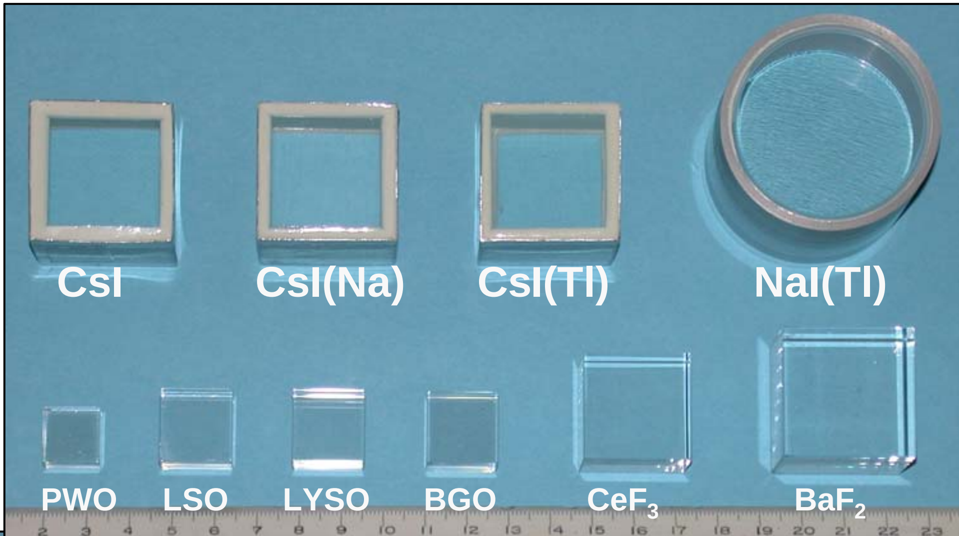

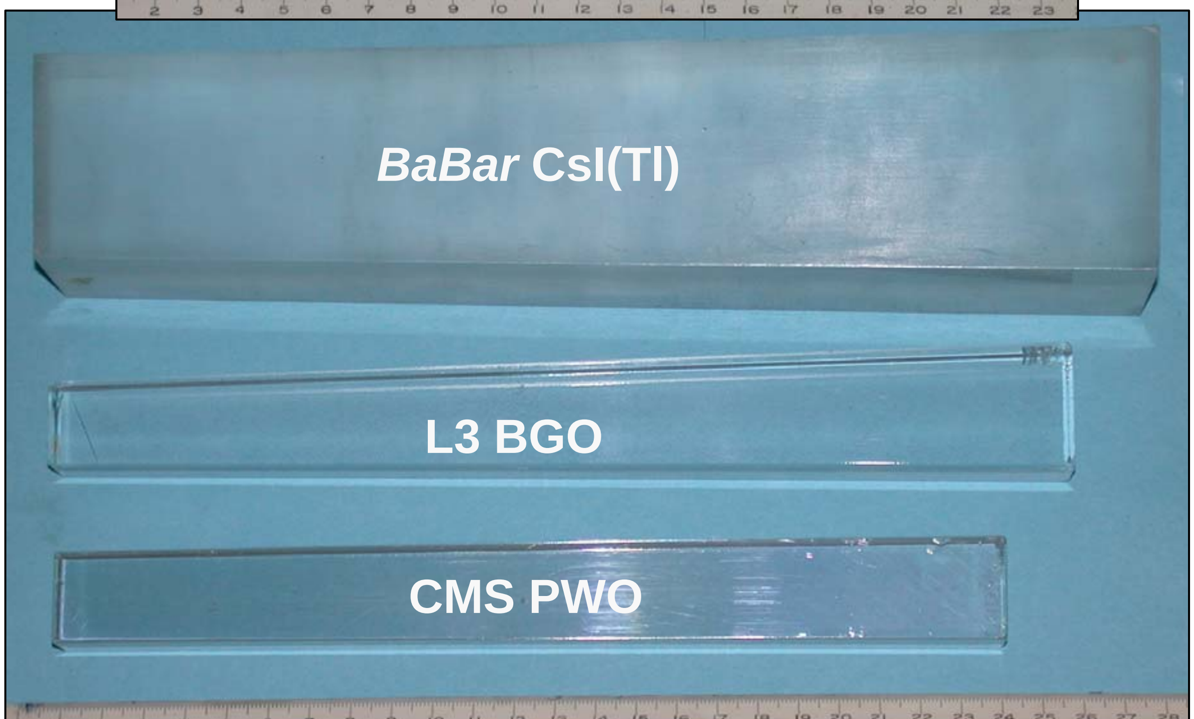

$1.5\ X_0$ Samples:

Hygroscopic Halides

Non-hygroscopic

Full Size Crystals:

BaBar CsI(Tl): $16\ X_0$

L3 BGO: $22\ X_0$

CMS PWO(Y): $25\ X_0$

Excitation, Emission & Transmission

$$T_s = (1-R)^2 + R^2(1-R)^2 + ... = (1-R)/(1+R), \text{ with}$$

$$R = \frac{(n_{crystal} - n_{air})^2}{(n_{crystal} + n_{air})^2}.$$

Theoretical limit of transmittance: NIM **A333** (1993) 422

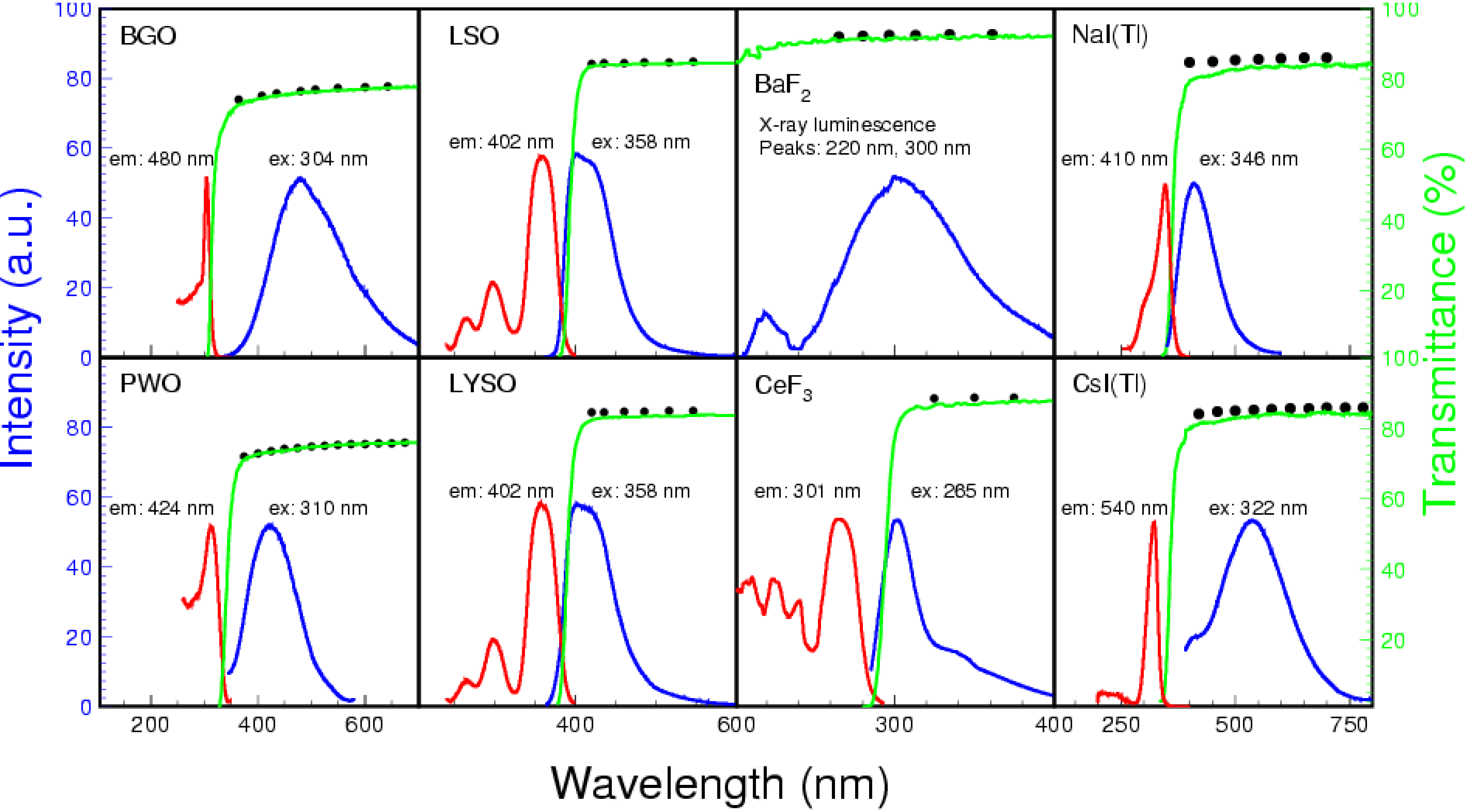

Scintillation Light Decay Time

Recorded with an Agilent 6052A digital scope

Fast Scintillators

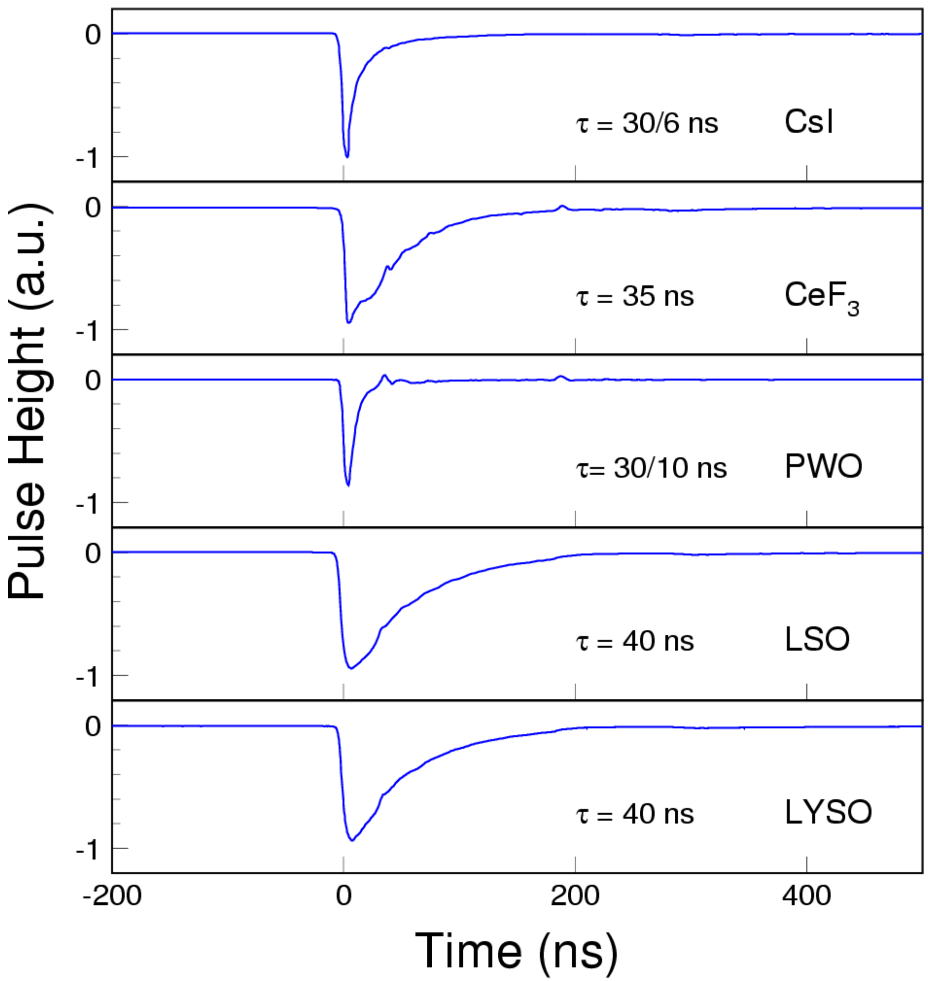

Slow Scintillators

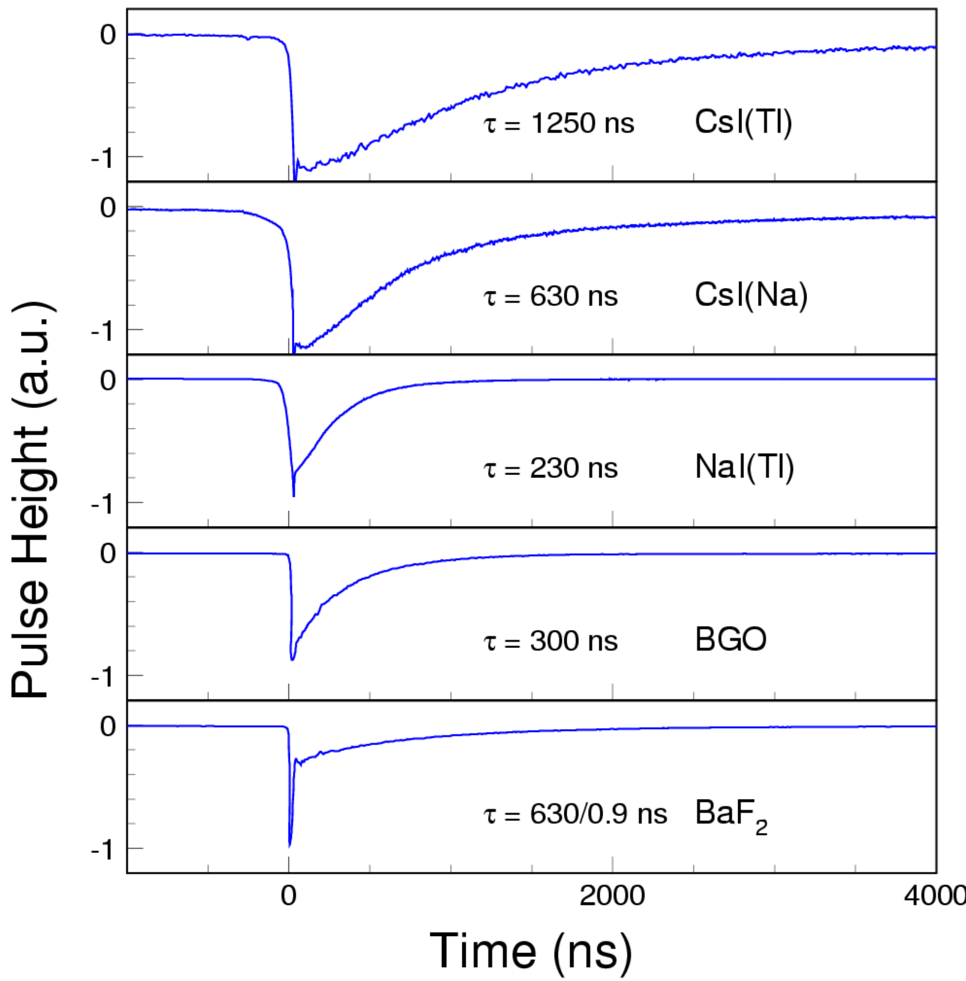

Scintillation Light Output

Measured with a Philips XP2254B PMT (multi-alkali cathode)
p.e./MeV: LSO/LYSO is 6 & 230 times of BGO & PWO respectively

Fast Scintillators

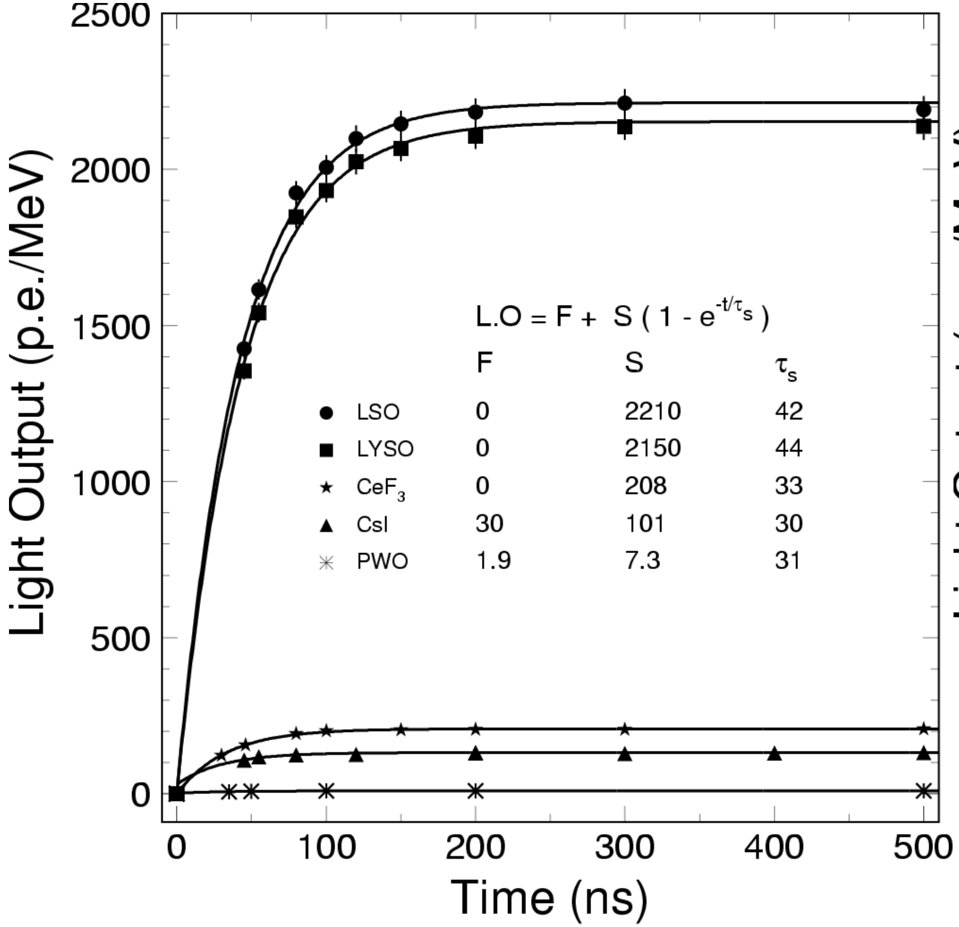

Slow Scintillators

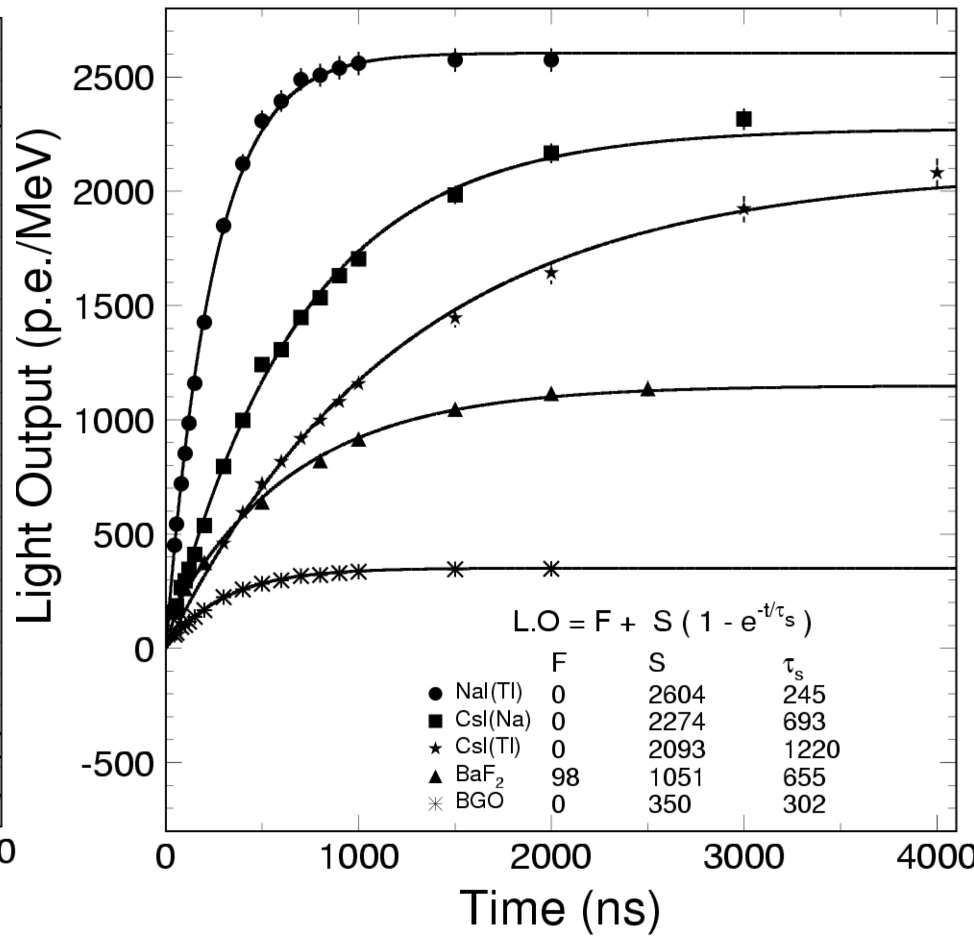

Emission weighted PMT Q.E.

Taking out QE, L.O. of LSO/LYSO is 4/220 times BGO/PWO
Hamamatsu S8664-55 APD has QE 75% for LSO/LYSO

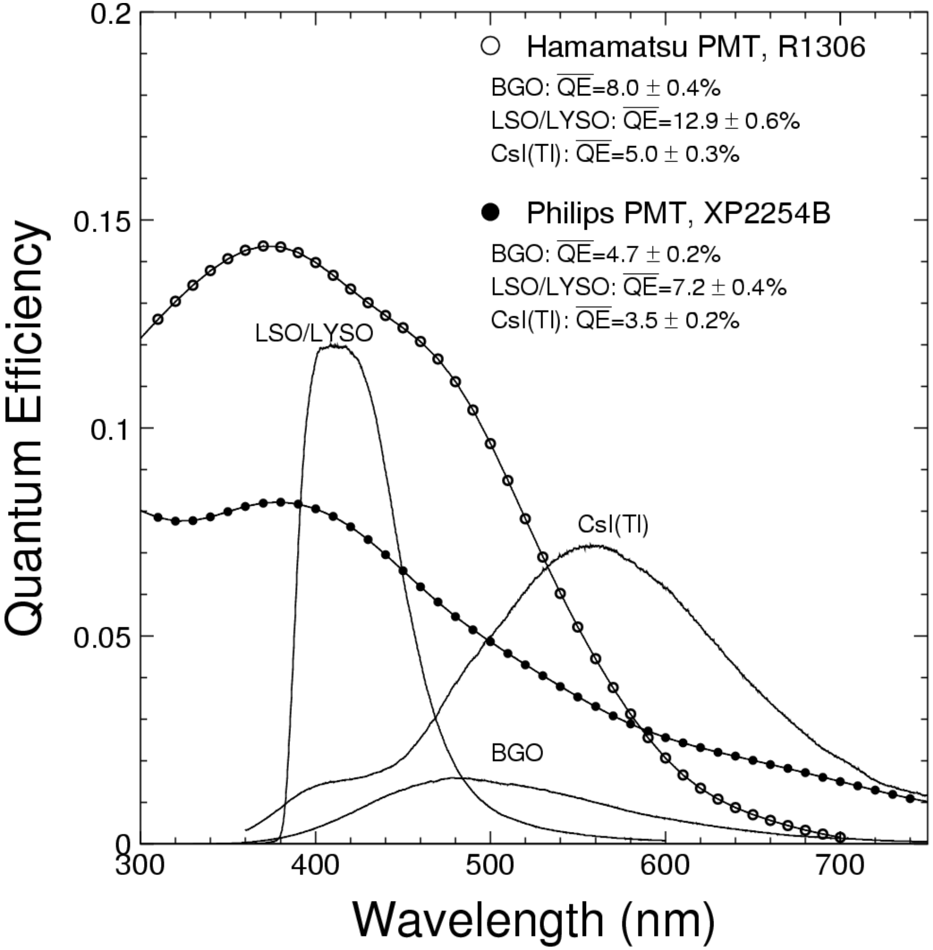

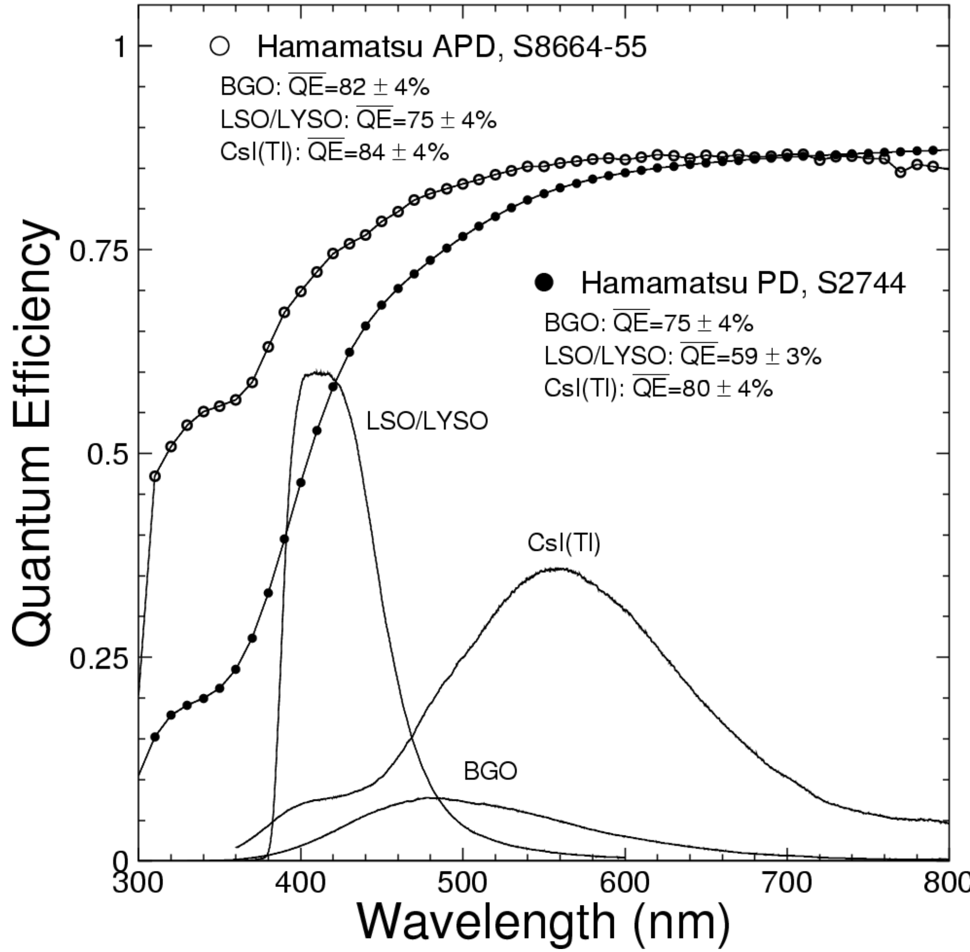

BGO, LSO & LYSO Samples

2.5 x 2.5 x 20 cm (18 X_0)

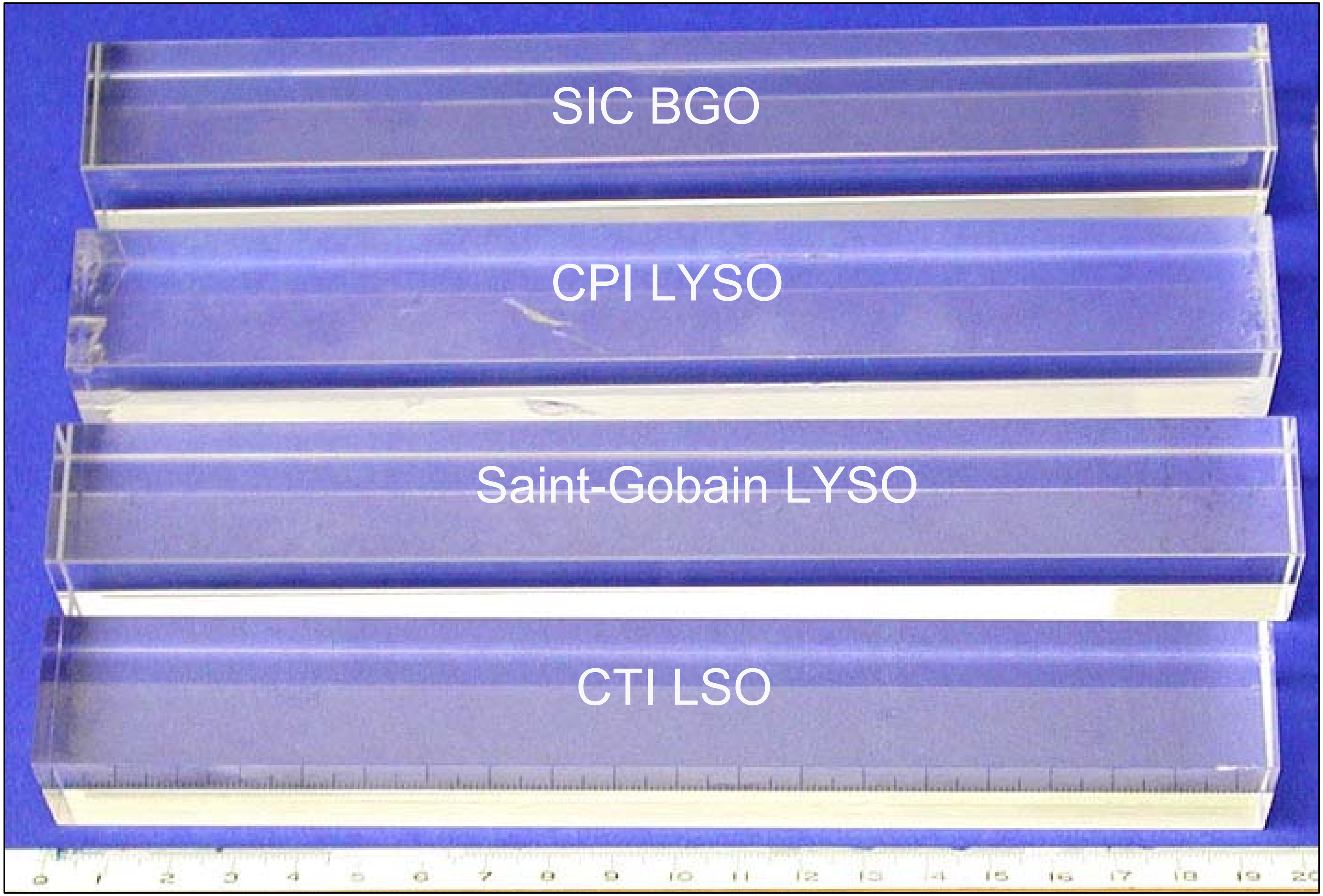

LSO/LYSO with PMT Readout

~10% FWHM resolution for ^{22}Na source (0.51 MeV)
1,200 p.e./MeV, 5/230 times of BGO/PWO

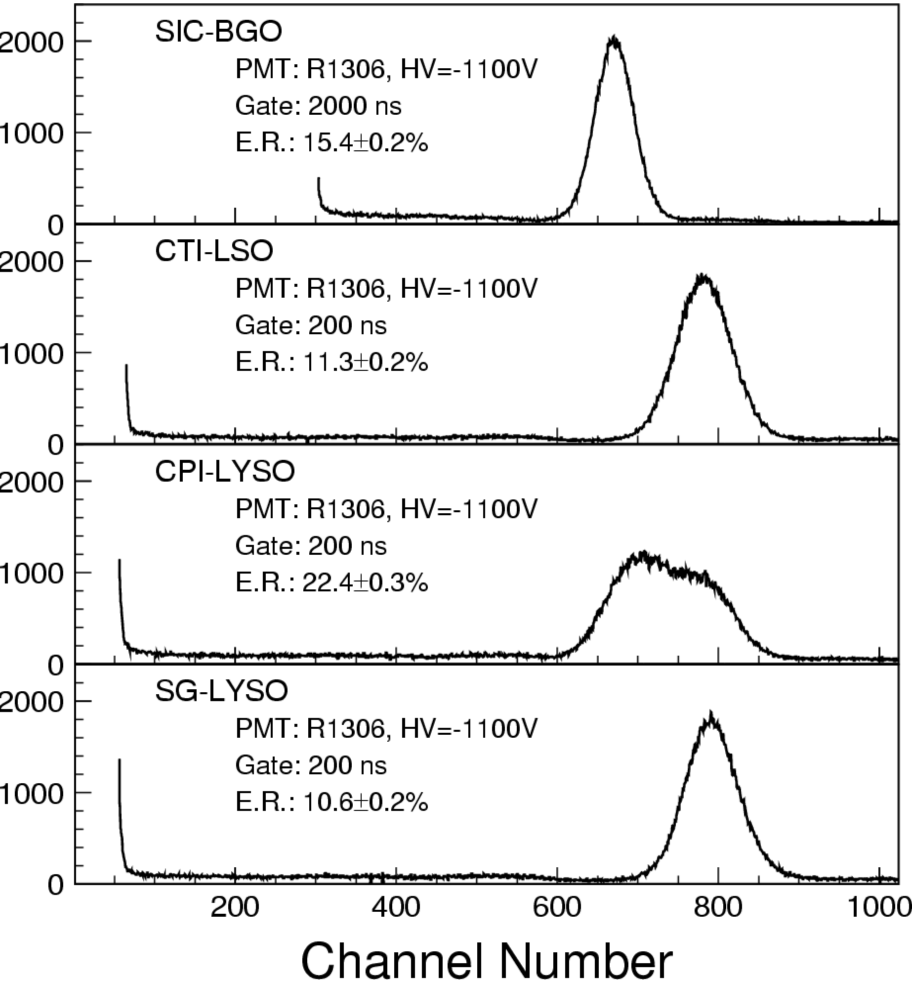

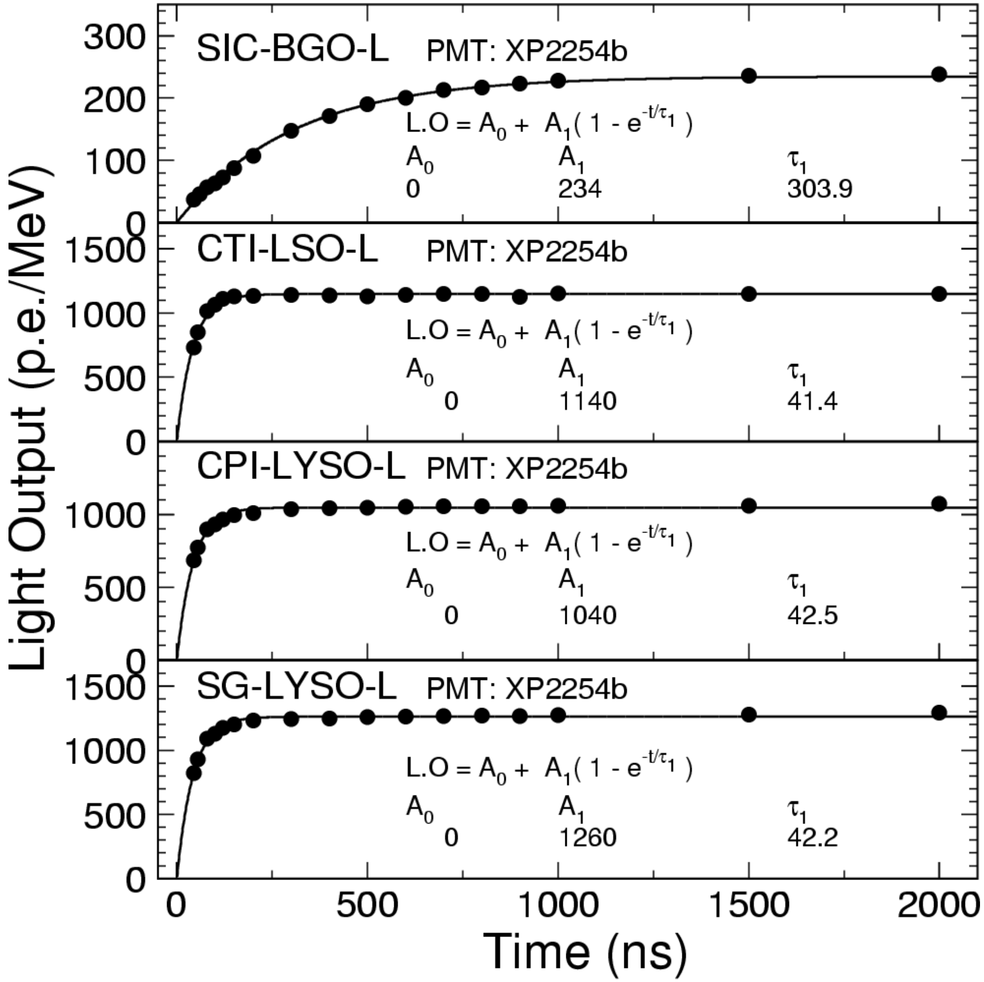

LSO/LYSO with APD Readout

L.O.: 1,500 p.e./MeV, 4/200 times of BGO/PWO
Readout Noise: <40 keV

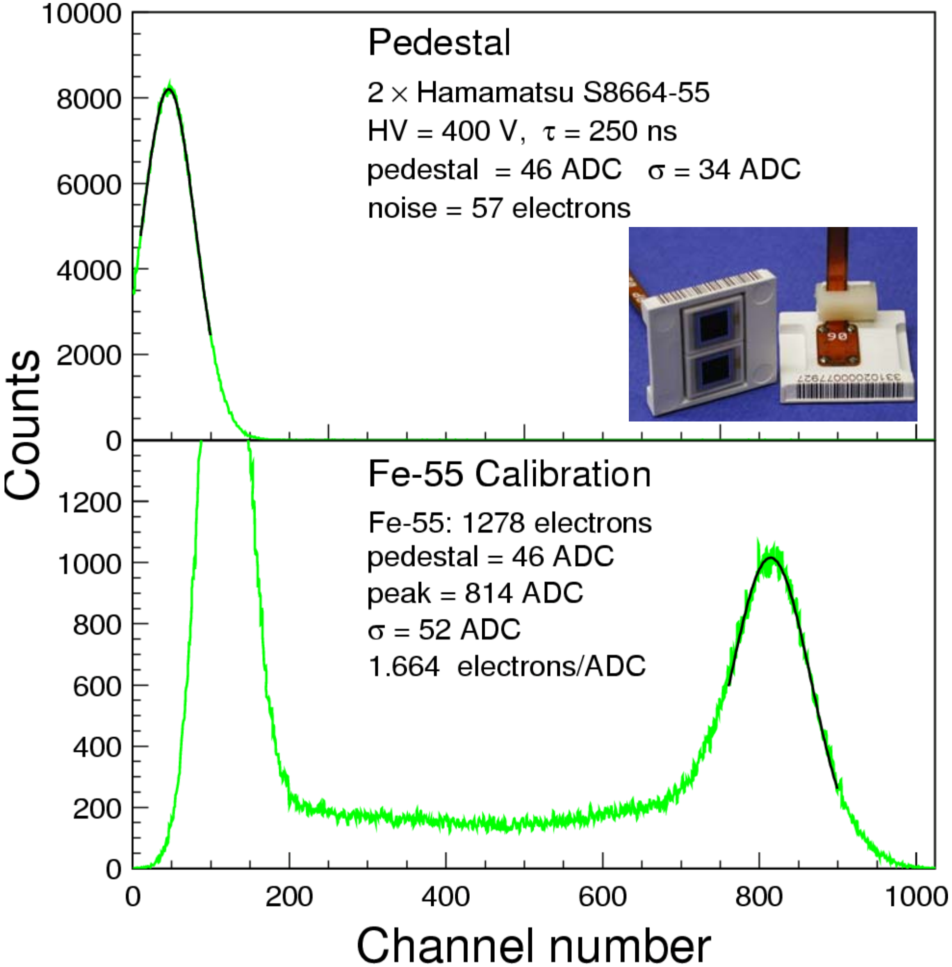

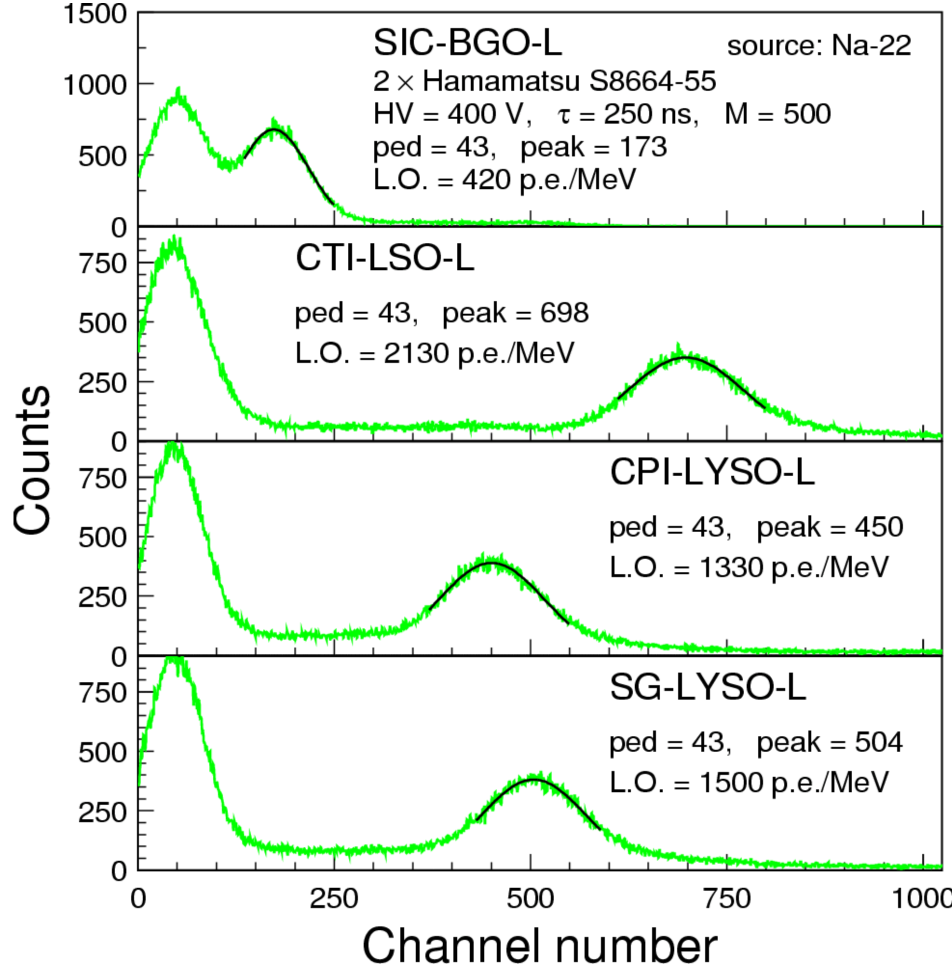

Crystal Calorimeters in HEP

Date	75-85	80-00	80-00	80-00	90-10	94-10	94-10	95-20
Experiment	C. Ball	L3	CLEO II	C. Barrel	KTeV	*BaBar*	BELLE	CMS
Accelerator	SPEAR	LEP	CESR	LEAR	FNAL	SLAC	KEK	CERN
Crystal Type	NaI(Tl)	BGO	CsI(Tl)	CsI(Tl)	CsI	CsI(Tl)	CsI(Tl)	$PbWO_4$
B-Field (T)	-	0.5	1.5	1.5	-	1.5	1.0	4.0
r_{inner} (m)	0.254	0.55	1.0	0.27	-	1.0	1.25	1.29
Number of Crystals	672	11,400	7,800	1,400	3,300	6,580	8,800	76,000
Crystal Depth (X_0)	16	22	16	16	27	16 to 17.5	16.2	25
Crystal Volume (m^3)	1	1.5	7	1	2	5.9	9.5	11
Light Output (p.e./MeV)	350	1,400	5,000	2,000	40	5,000	5,000	2
Photosensor	PMT	Si PD	Si PD	WS[a]+Si PD	PMT	Si PD	Si PD	APD[a]
Gain of Photosensor	Large	1	1	1	4,000	1	1	50
σ_N/Channel (MeV)	0.05	0.8	0.5	0.2	small	0.15	0.2	40
Dynamic Range	10^4	10^5	10^4	10^4	10^4	10^4	10^4	10^5

Future crystal calorimeters in HEP:

PANDA at GSI: PWO or BGO?

LSO/LYSO for a Super B Factory or ILC?

L3 BGO Resolution

Contribution	“Radiative”+Intrinsic	Temperature	Calibration	Overall
Barrel	0.8%	0.5%	0.5%	1.07%
Endcaps	0.6%	0.5%	0.4%	0.88%

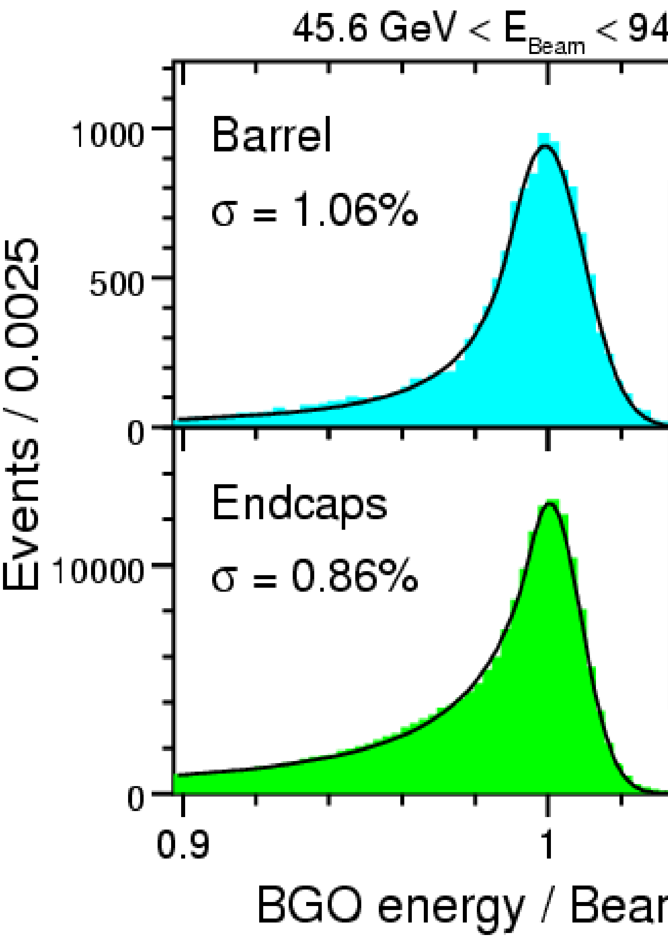

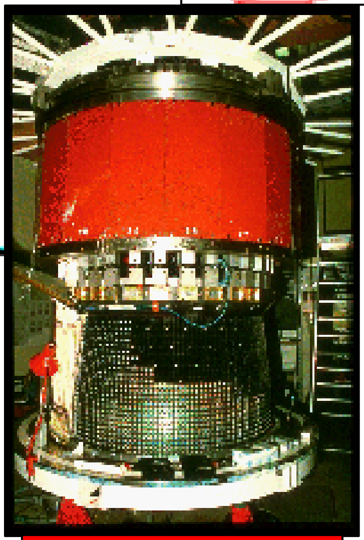

12k BGO

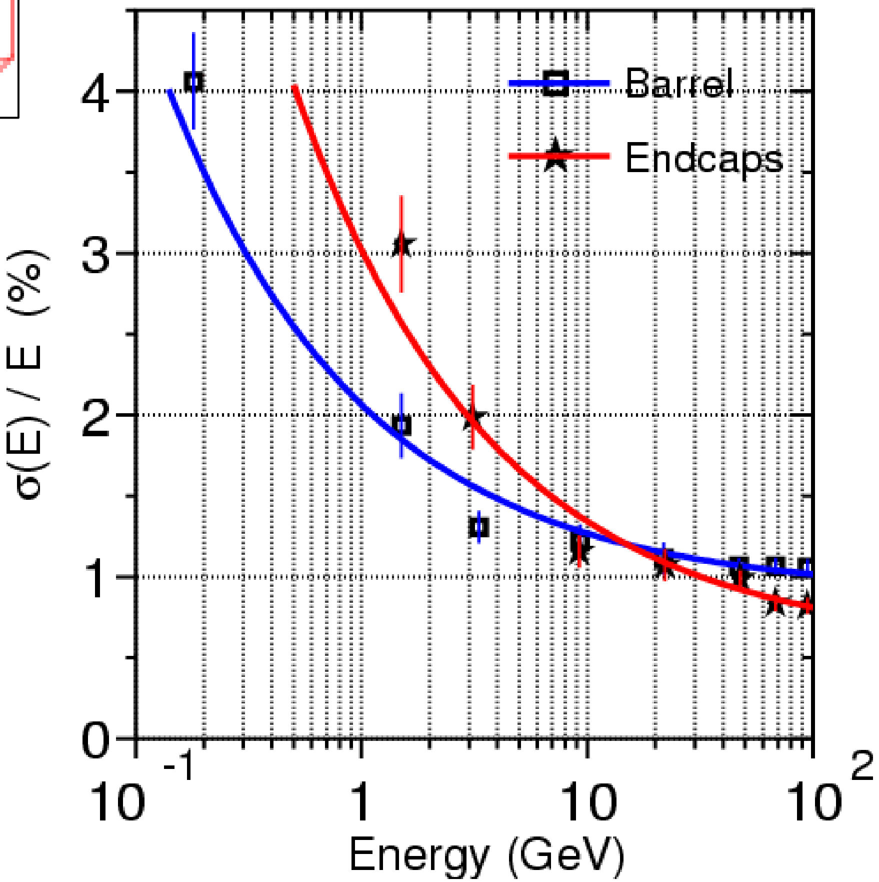

KTeV CsI Position Resolution

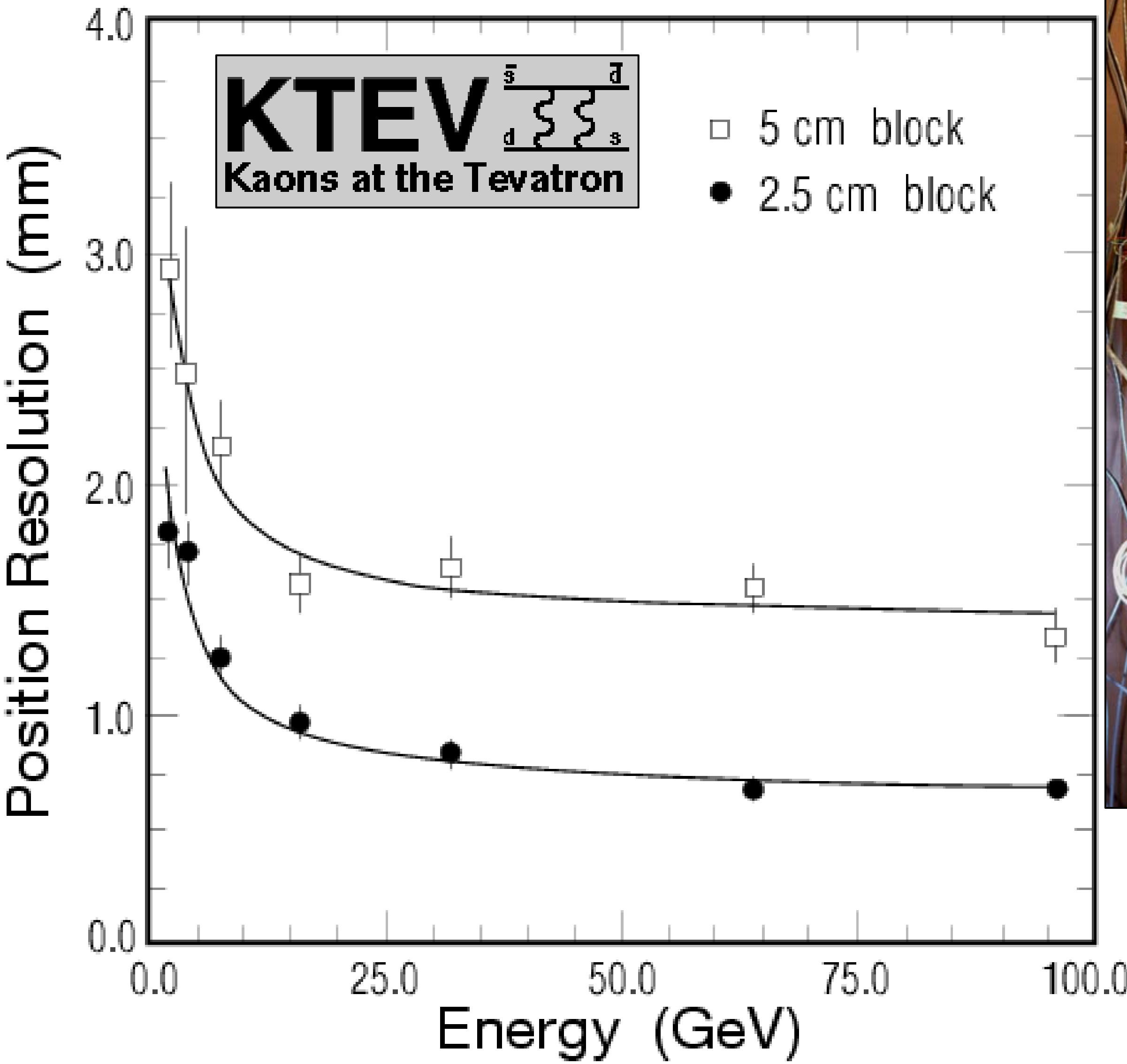

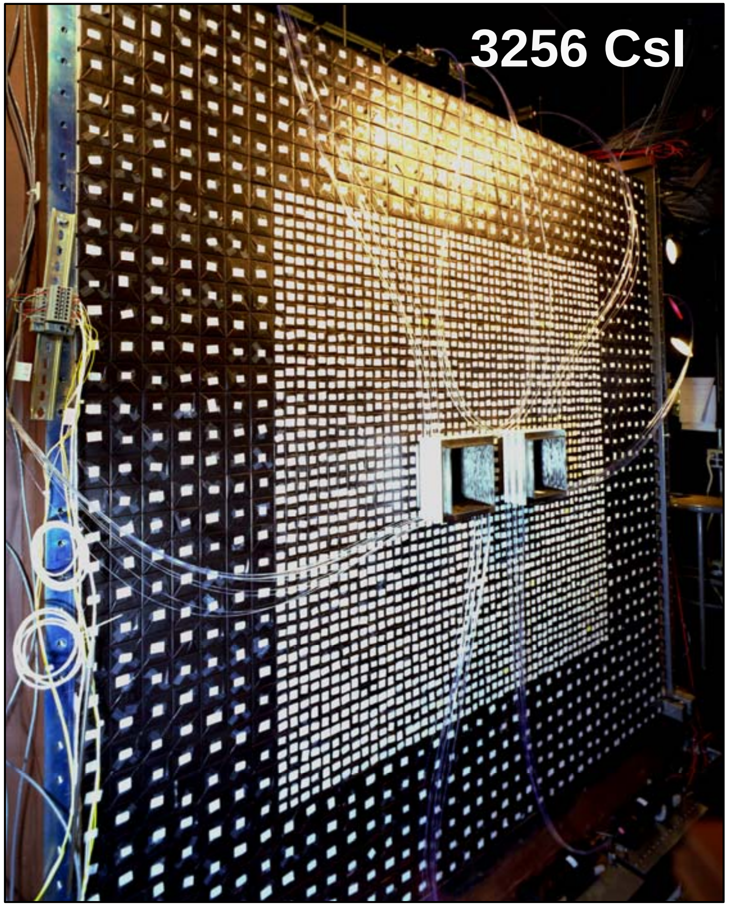

Sub mm position resolution.
L3 BGO & CMS PWO: 0.3 mm.

BaBar CsI(Tl) Resolution

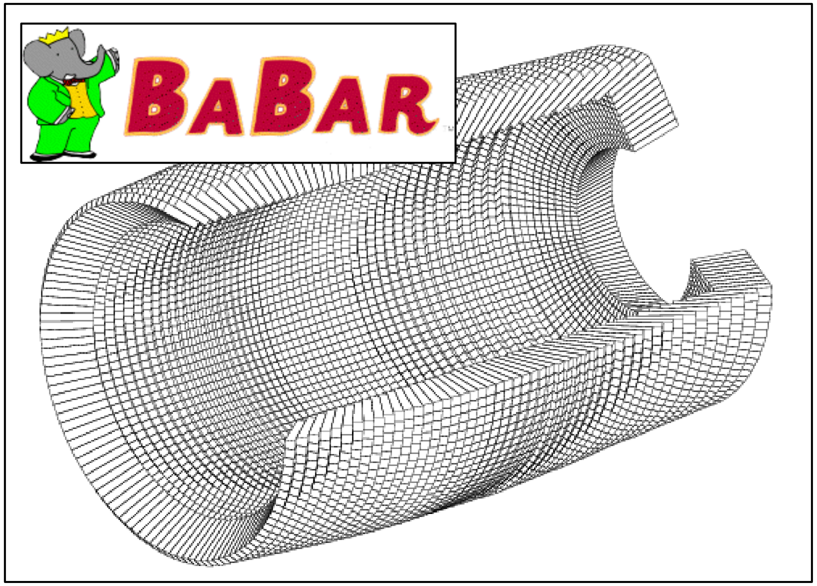

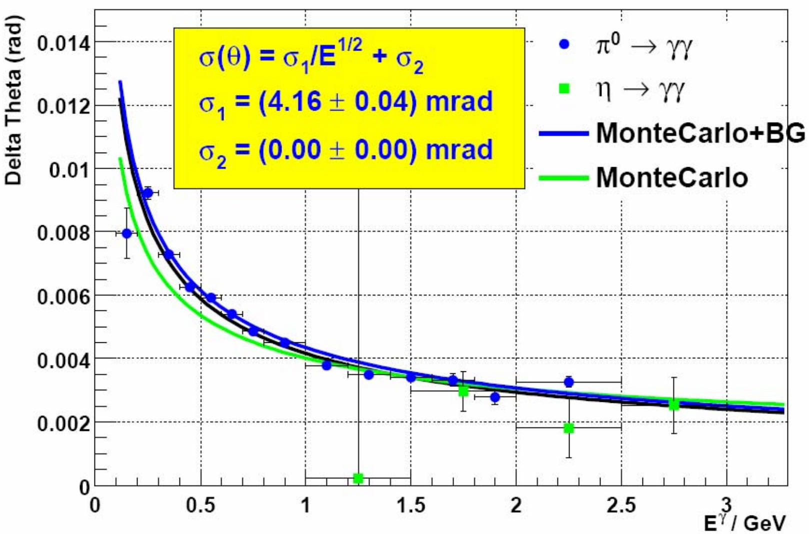

Energy resolution

M. Kocian, SLAC, CALOR2002

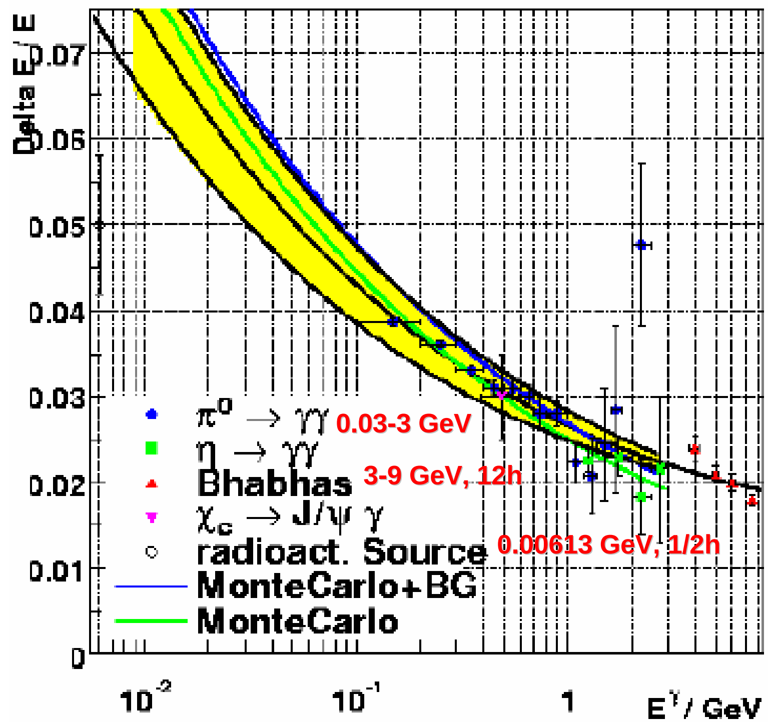

$$\frac{\sigma_E}{E} = \frac{\sigma_1}{\sqrt[4]{E}} \oplus \sigma_2$$

$$\sigma_1 = (2.30 \pm 0.03 \pm 0.3)\%$$

$$\sigma_2 = (1.35 \pm 0.08 \pm 0.2)\%$$

PWO Crystal ECAL Resolution

Crystal Aging & Radiation Damage?

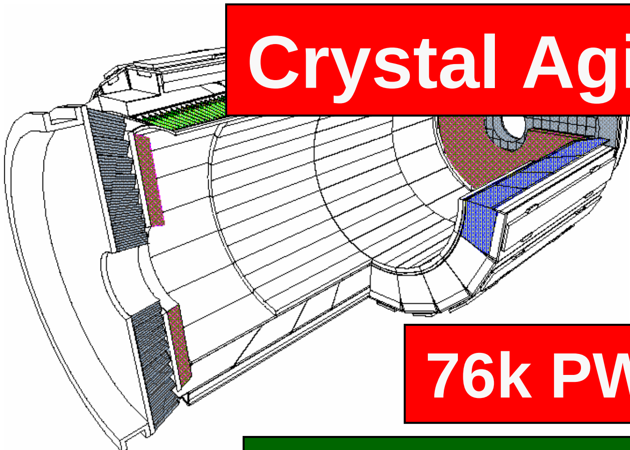

76k PWO

Measured Resolution

$\sigma(E)/E < 1\%$ if $E > 25$ GeV

$\sigma(E)/E \sim 0.5\%$ at 120 GeV

Designed Resolution

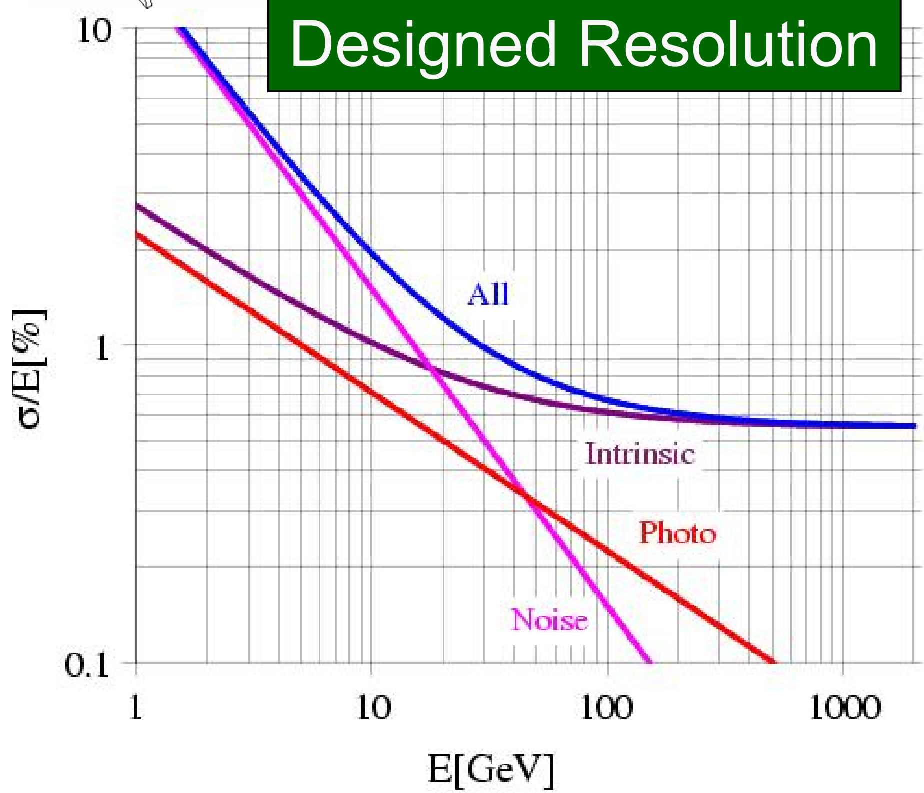

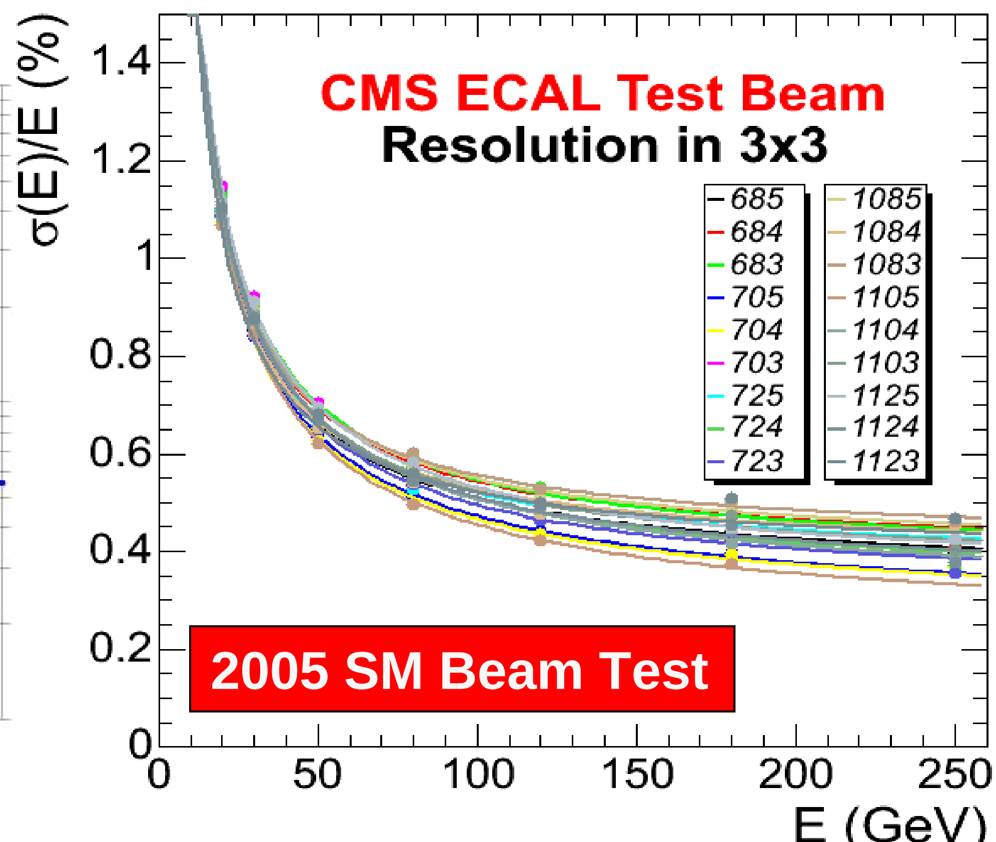

2005 SM Beam Test

Crystal Degradation *in situ*

L3 BGO degrades 6 – 7% in 7 years

BaBar CsI(Tl): 1 - 3 % per year

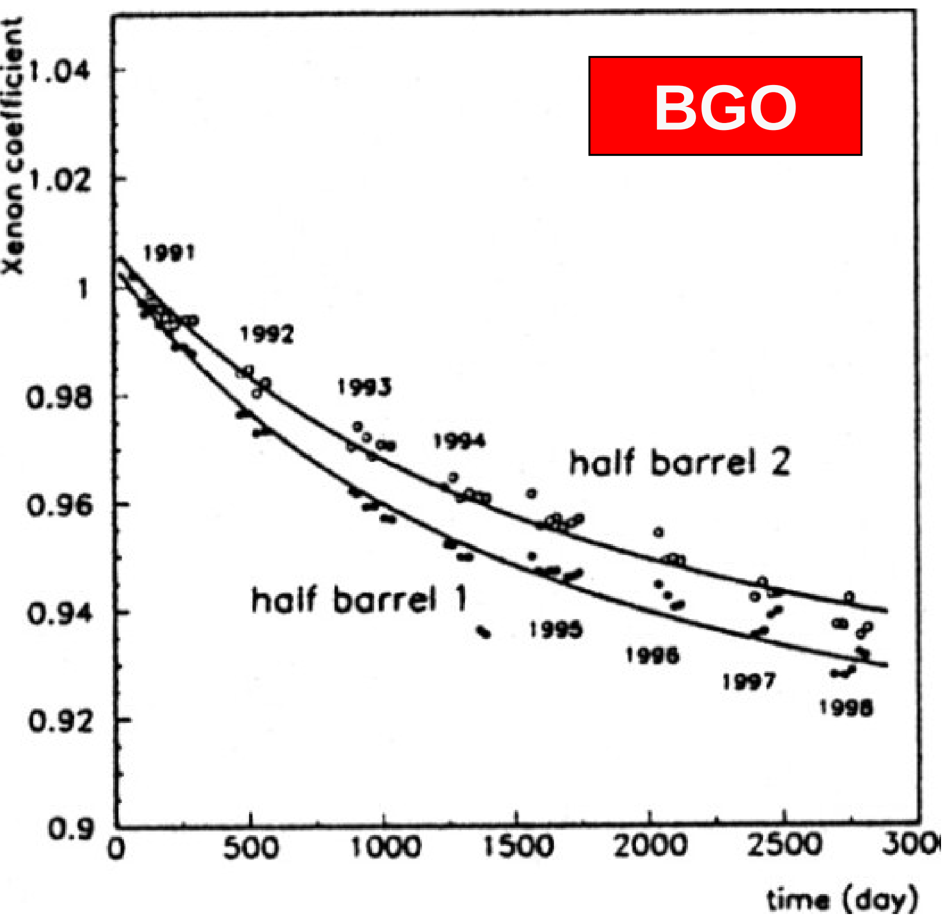

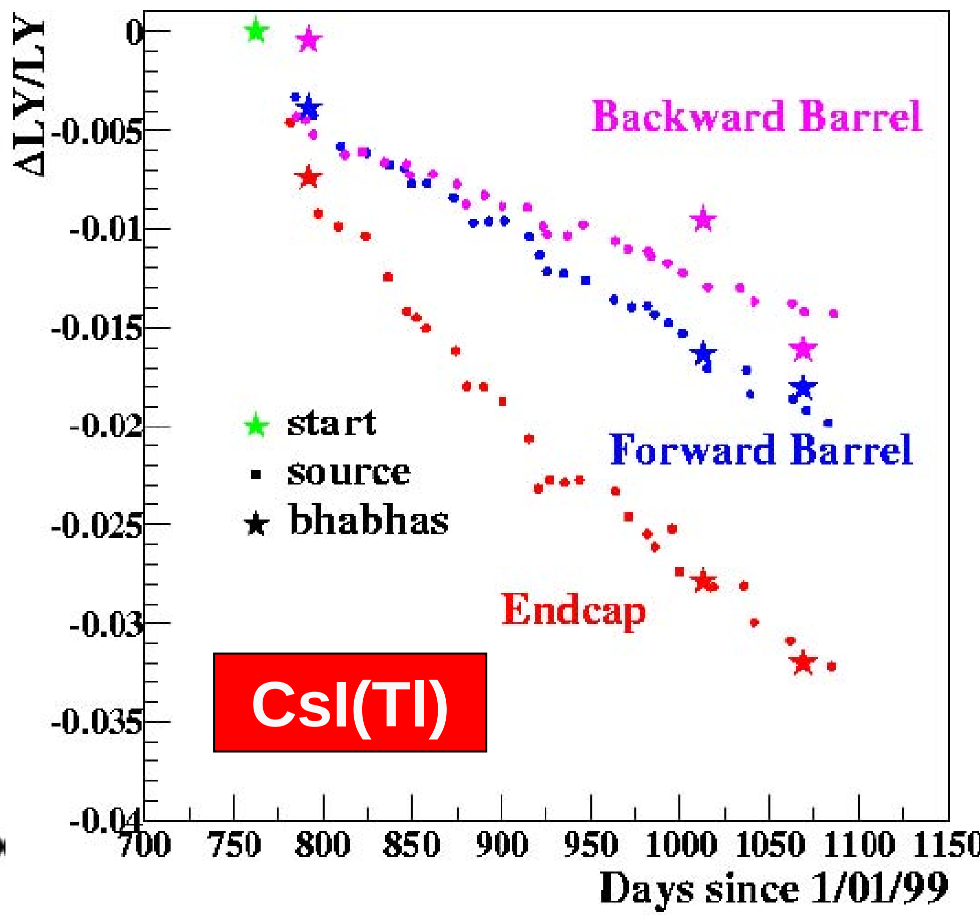

Effects of Radiation Damage

- Induced absorption caused by color center formation:
  - reduced light attenuation length and thus light output, and maybe
  - degraded of light response uniformity (LRU).
- Induced phosphorescence:
  - increase readout noise.
- Reduced scintillation light yield:
  - reduce light output and degrade light response uniformity.

Item	CsI(Tl)	CsI	BaF_2	BGO	$PbWO_4$
Color Centers	Yes	Yes	Yes	Yes	Yes
Fluorescence	Yes	Yes	Yes	Yes	Yes
Scintillation	No	No	No	No	No
Recover @RT	Slow	Slow	No	Yes	Yes
Dose Rate Dependence	No	No	No	Yes	Yes
Thermall Annealing	No/Yes	No/Yes	Yes	Yes	Yes
Optical Bleaching	No/Yes	No/Yes	Yes	Yes	Yes

Radiation Induced Absorption

Measured with Hitachi U-3210 Photospectrometer

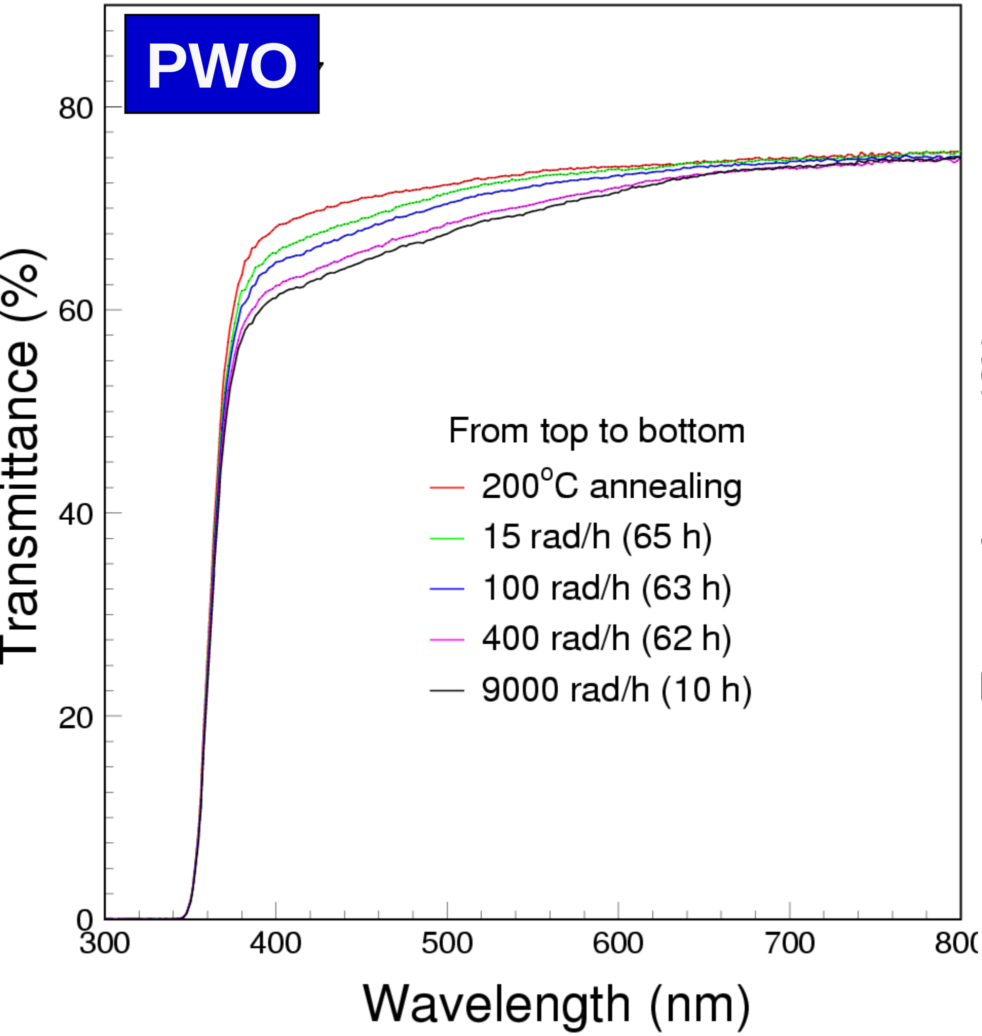

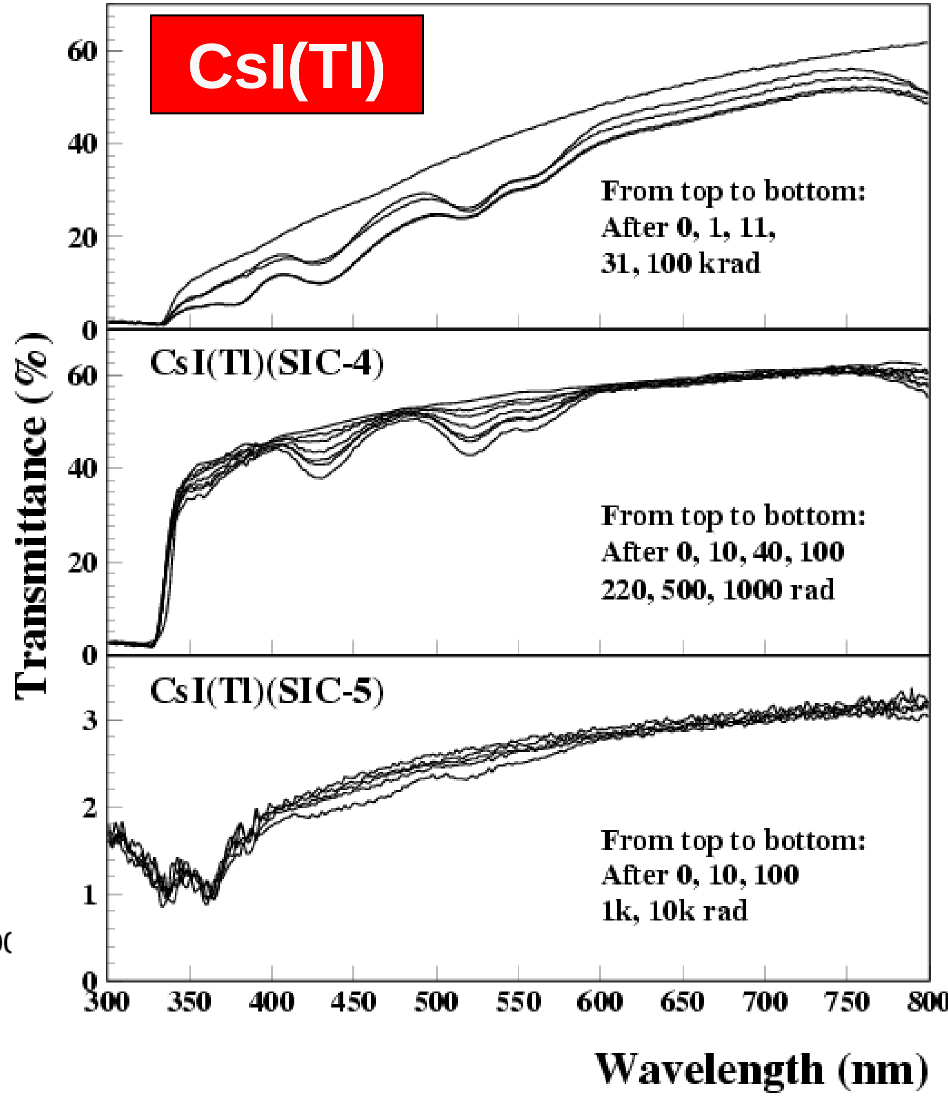

SIMS Study & CsI(Tl) Improvement

Secondary Ion Mass Spectroscopy revealed depth profile of oxygen contamination; Oxygen control improves CsI(Tl) quality

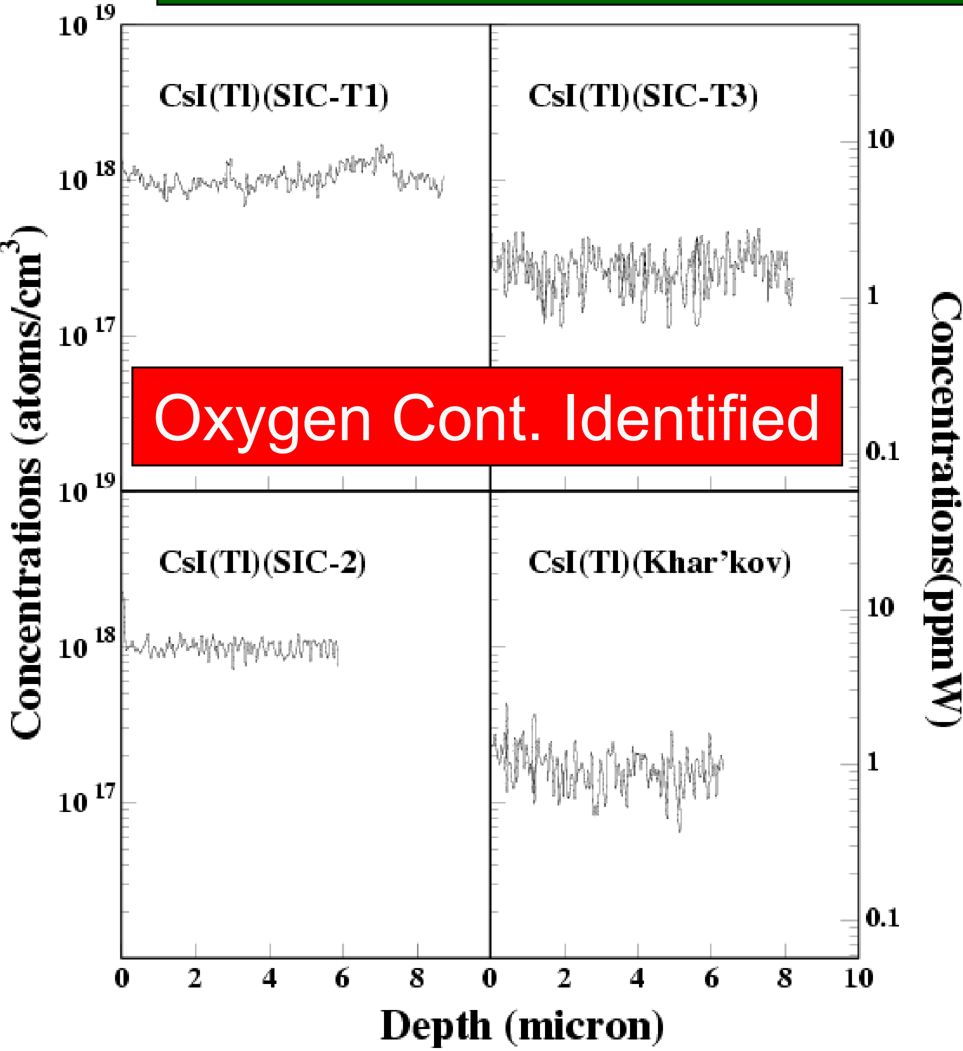

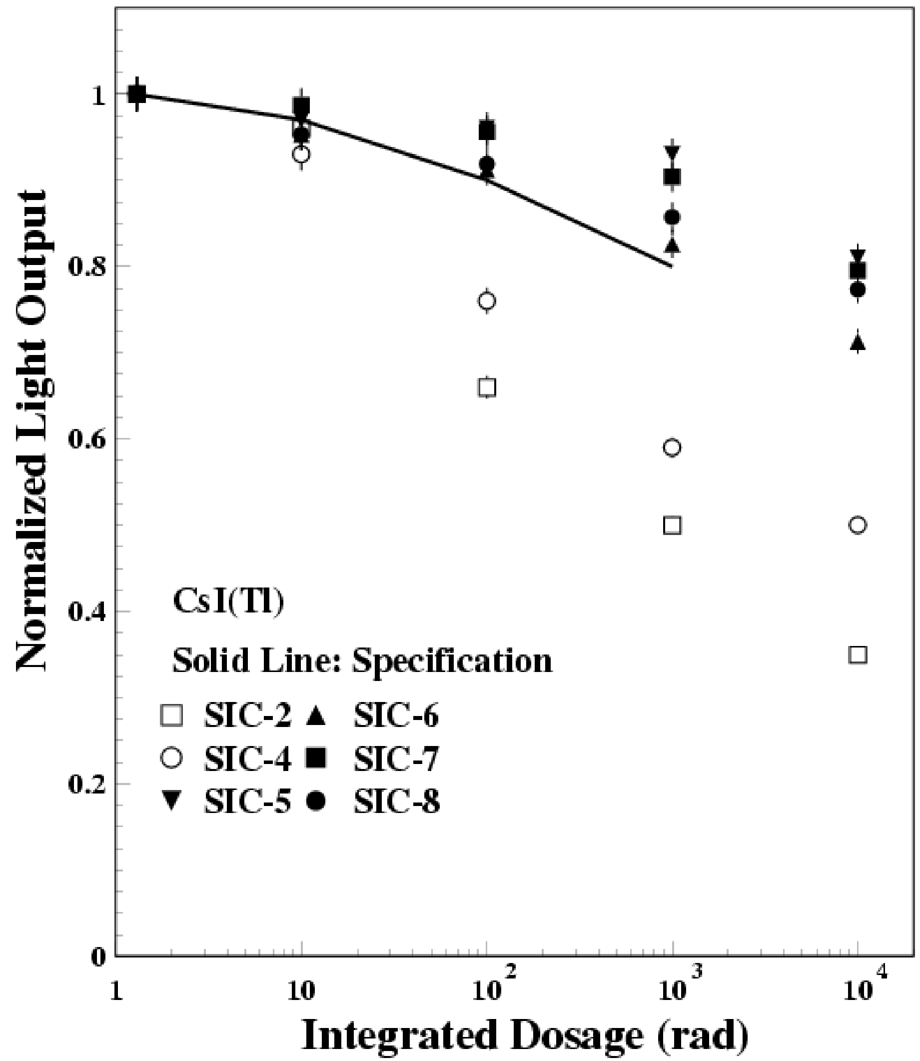

TEM/EDS Study on PWO Crystals

TOPCON-002B scope, 200 kV, 10 uA, 5 to10 nm black spots identified
JEOL JEM-2010 scope and Link ISIS EDS localized Stoichiometry Analysis

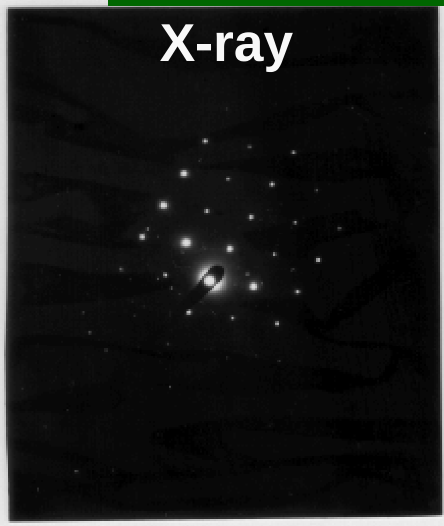

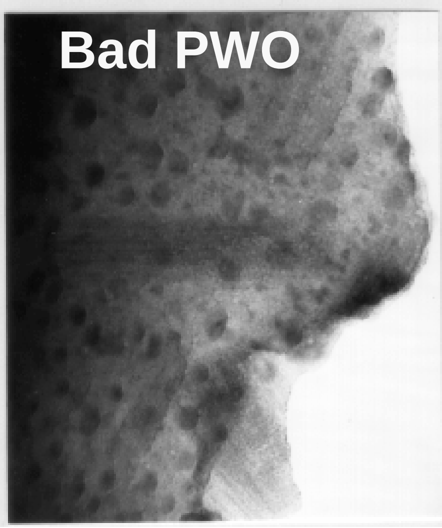

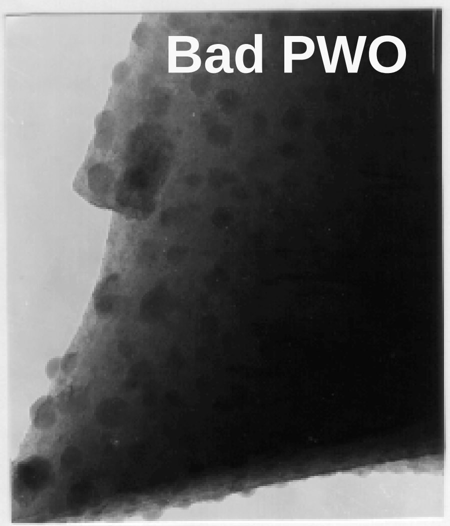

Atomic Fraction (%) in $PbWO_4$

As Grown Sample

Element	Black Spot	Peripheral	$Matrix_1$	$Matrix_2$
O	1.5	15.8	60.8	63.2
W	50.8	44.3	19.6	18.4
Pb	47.7	39.9	19.6	18.4

The Same Sample after Oxygen Compensation

Element	$Point_1$	$Point_2$	$Point_3$	$Point_4$
O	59.0	66.4	57.4	66.7
W	21.0	16.5	21.3	16.8
Pb	20.0	17.1	21.3	16.5

Oxygen Vacancies Identified

BGO/PWO Quality Improvement

Nucl. Instr. and Meth. A302 (1991) 69

Nucl. Instr. and Meth. A480 (2002) 470

BGO damage recovery after 2.5 krad

PWO damage at different dose rate

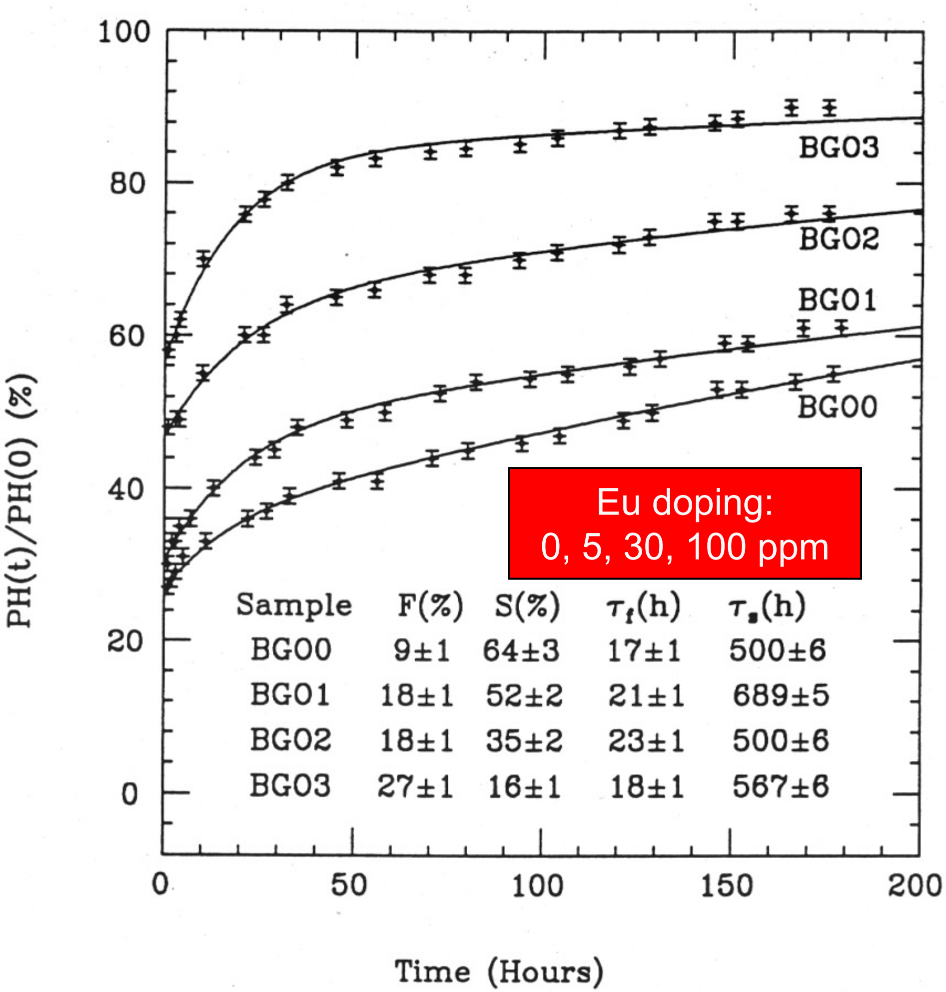

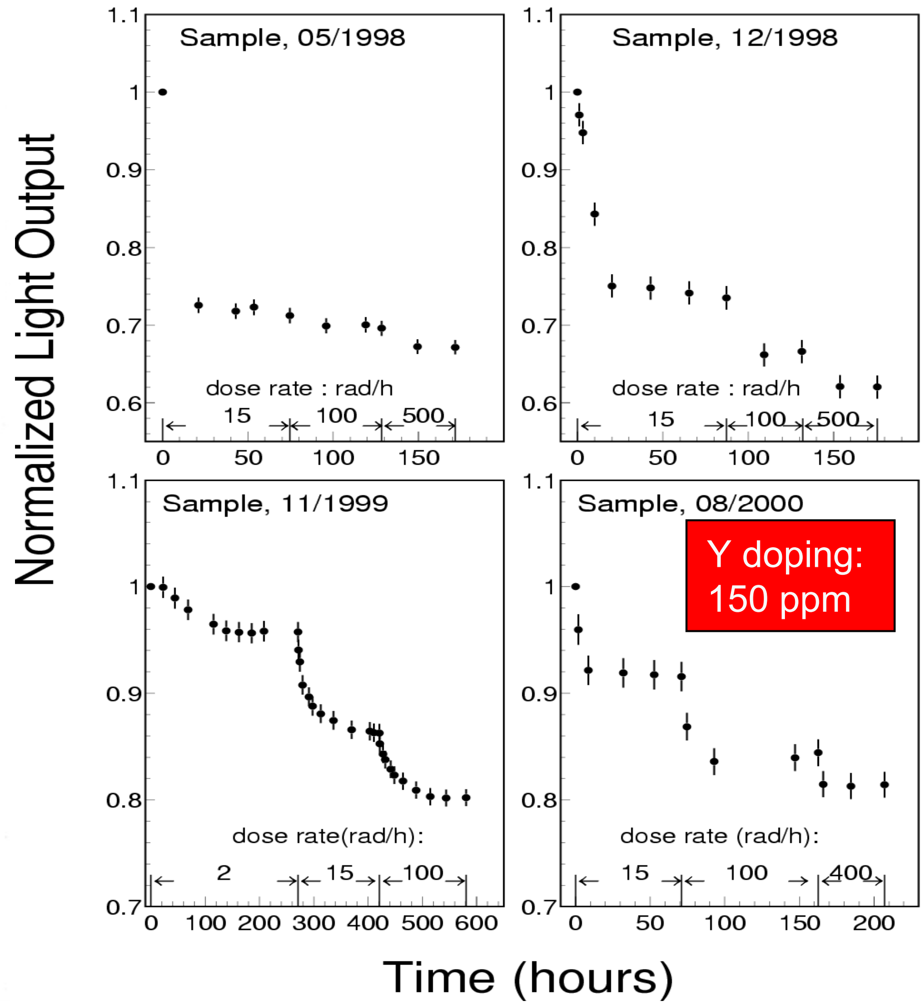

LYSO Transmittance Damage

LT @ 430 nm shows 6 and 3% increase under 2 rad/h, followed by 6 and 5% degradation under 9 krad/h for CPI and SG samples respectively

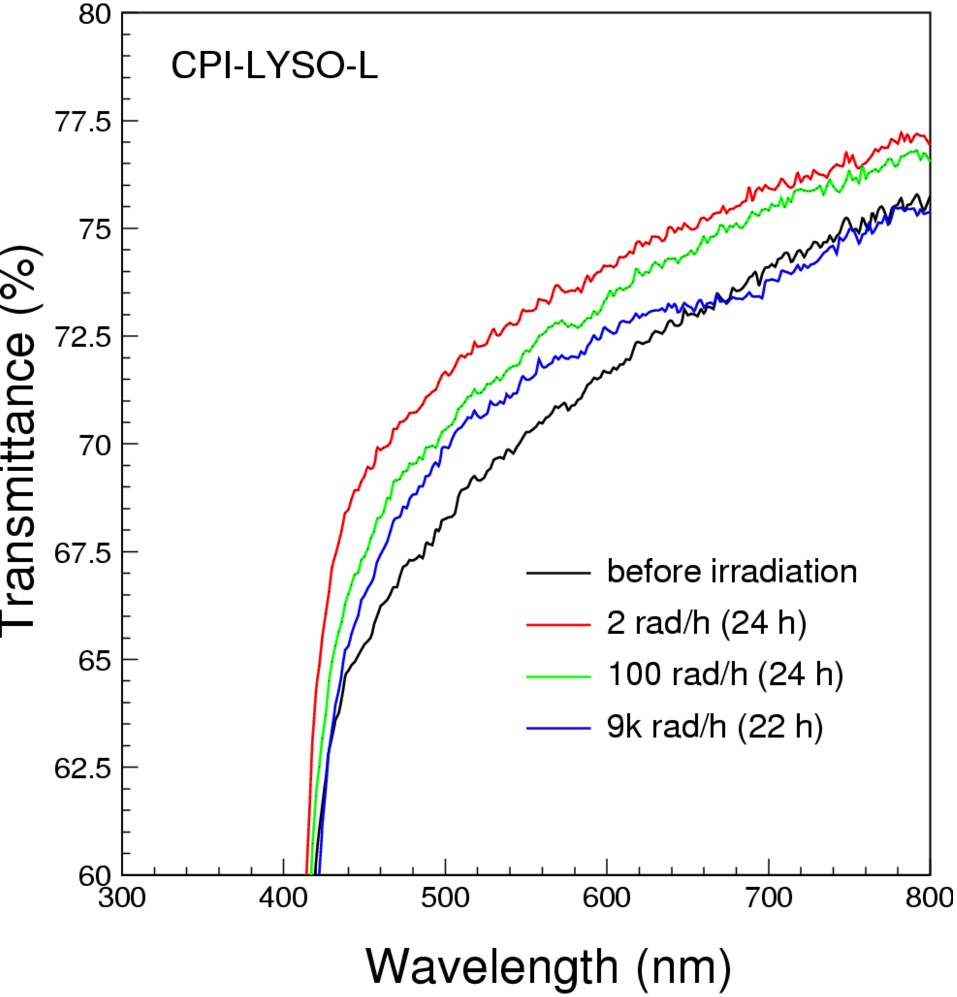

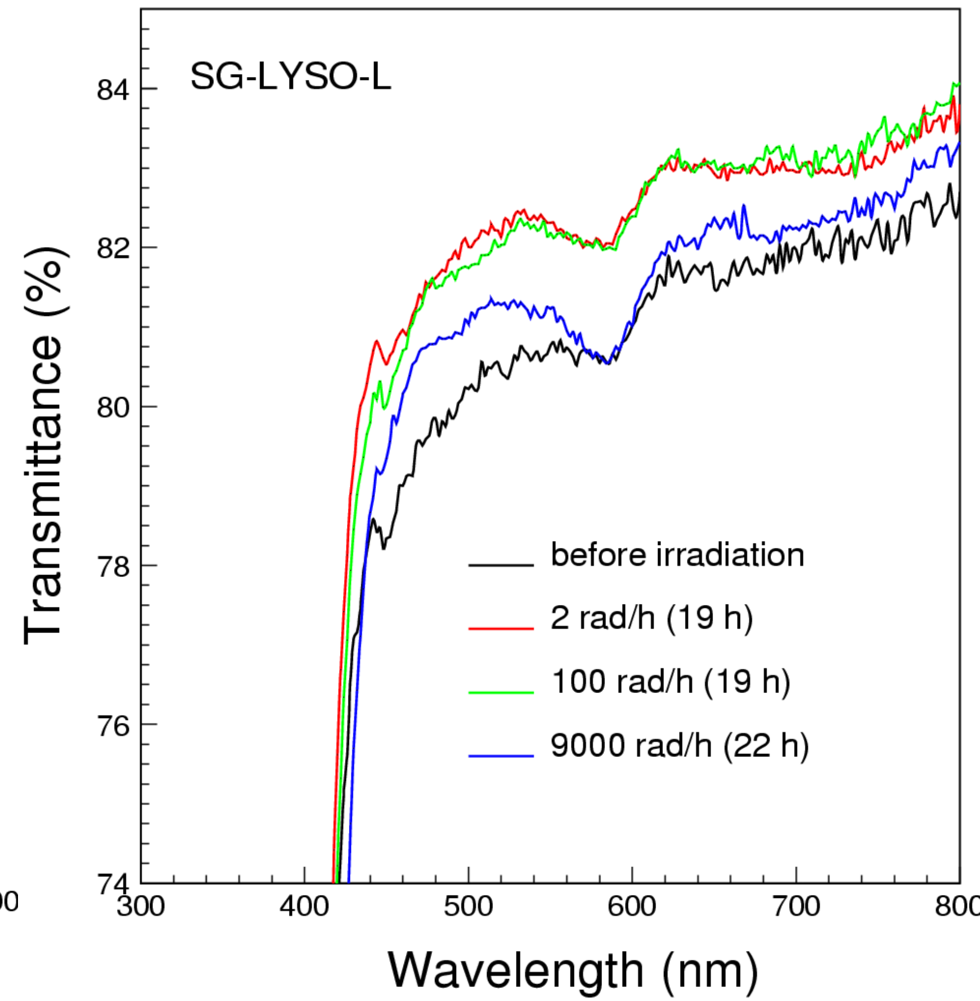

LSO/LYSO ECAL Performance

- Less demanding to the environment because of small temperature coefficient.
- Radiation damage is less an issue as compared to the CMS PWO ECAL.
- A better energy resolution, $\sigma(E)/E$, at low energies than L3 BGO and CMS PWO because of its high light output and low readout noise:

$$2.0\% / \sqrt{E} \oplus 0.5\% \oplus .001/E$$

Summary

- Because of total absorption, precision crystal calorimetry provides the best possible energy and position resolutions for electrons and photons as well as good e/γ identification and reconstruction efficiencies.
- Progress has been made in understanding crystal radiation damage and improving qualities of mass produced crystals.
- An LSO/LYSO crystal calorimeter will provide excellent energy resolution over a large dynamic range down to MeV level for future HEP and NP experiments.

Laser Monitoring for CMS ECAL

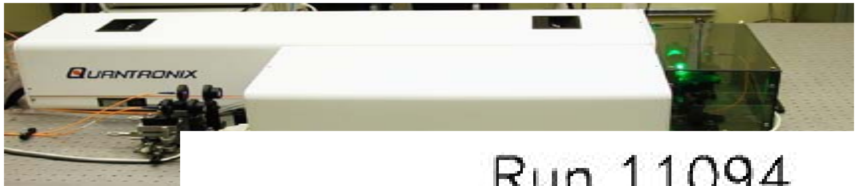

Tracking damage and recovery with laser light

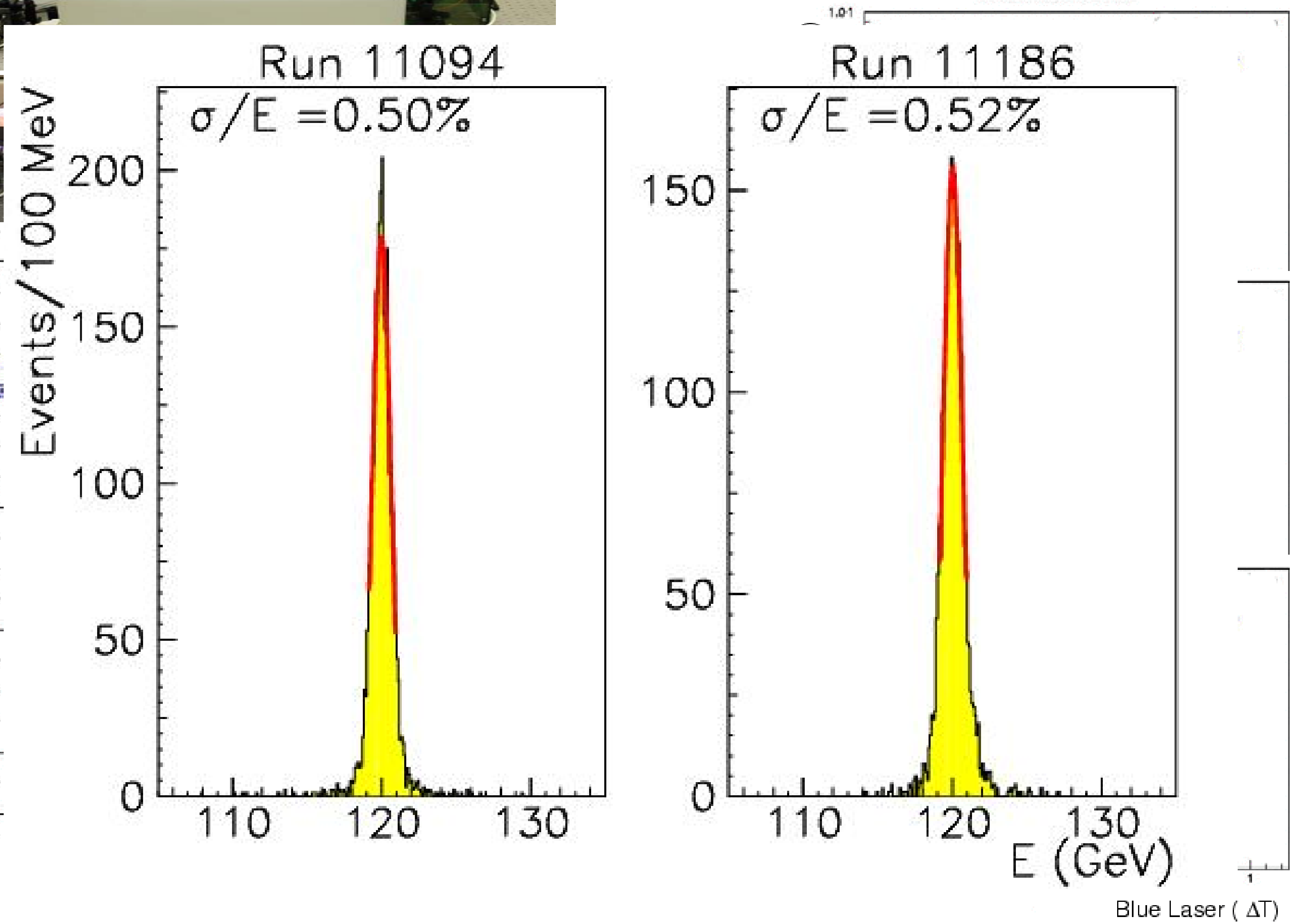

Light Response Uniformity (LRU)

Nucl. Instr. And Meth. A340 (1994) 442

Definition

$$Y = Y_{mid}\,[1 + \delta(x/x_{mid} - 1)]$$

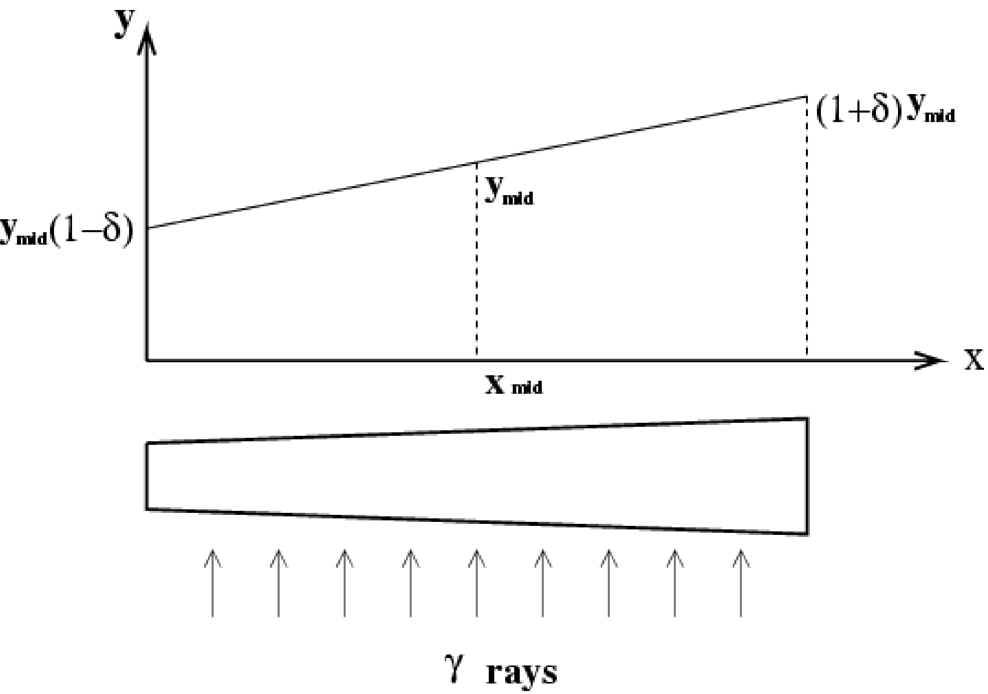

GEANT Simulation

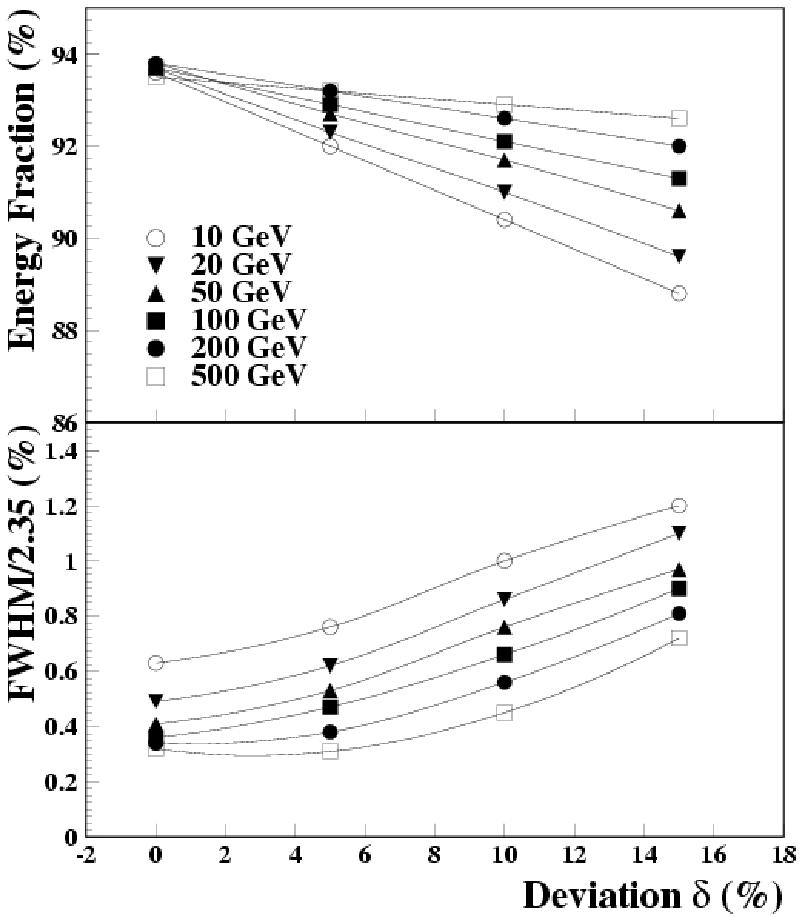

Resolution degradation is not recoverable if LRU is damaged

CMS Specification to the LRU

D. Graham & C. Seez, CMS Note 1996-002

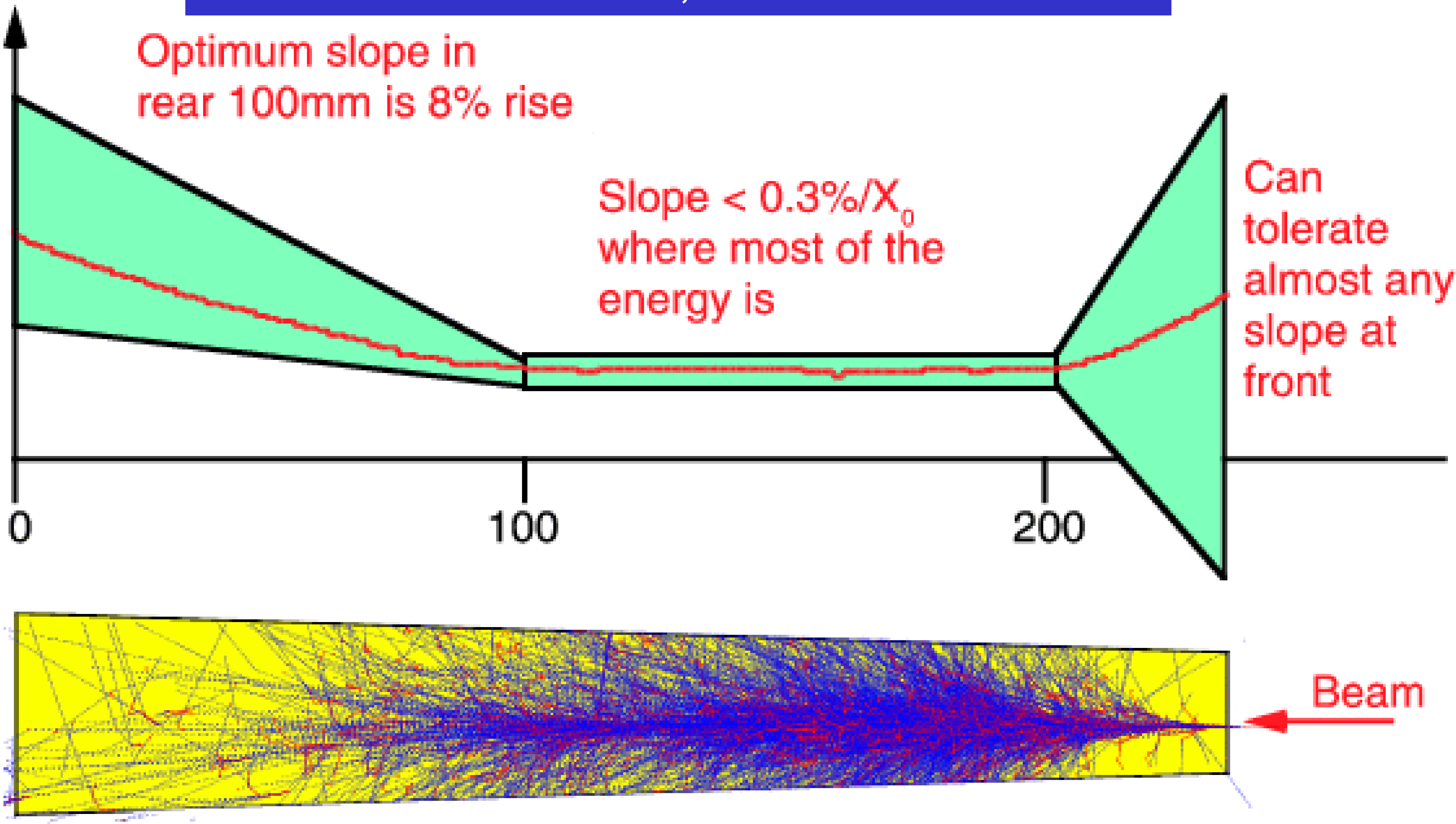

LAL affects LRU

Nucl. Instr. And Meth. A413 (1998) 297

Ray-Tracing simulation for CMS PWO crystals shows no change in LRU if LAL is longer than 3.5 crystal length

Light collection efficiency, fit to a linear function of distance to the small end of the crystal, was determined with two parameters: the light collection efficiency at the middle of the crystal and the uniformity.

LAL (cm)	20	40	60	80	200
Large Area Photo Detector, covering 100% back face					
η_m (%)	9.5±.2	15.7±.4	19.2±.5	21.6±.6	26.9±.7
δ (%)	23±1	-4.6±.8	-11±1	-15±1	-15±1
ϕ5 mm Photo Detector, covering 3.7% back face					
η_m (%)	.38±.04	.74±.08	1.1±.1	1.4±.2	3.0±.3
δ (%)	23±4	–3.5±4	-12±4	-16±4	-17±3
$\frac{\eta_m(\phi 5mm)}{\eta_m(Full)}$ (%)	4.0	4.7	5.7	6.5	11

PWO Radiation Damage

No damage in scintillation mechanism

No damage in resolution if light attenuation length > 1 m

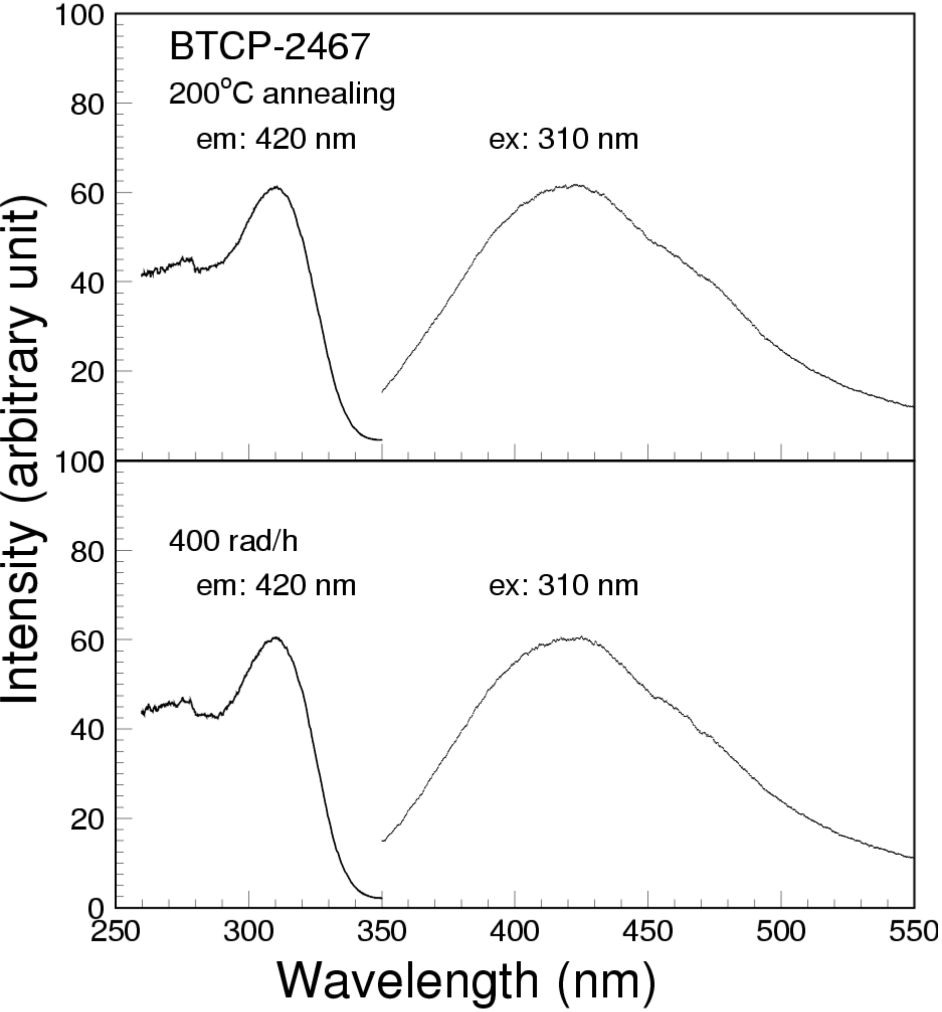

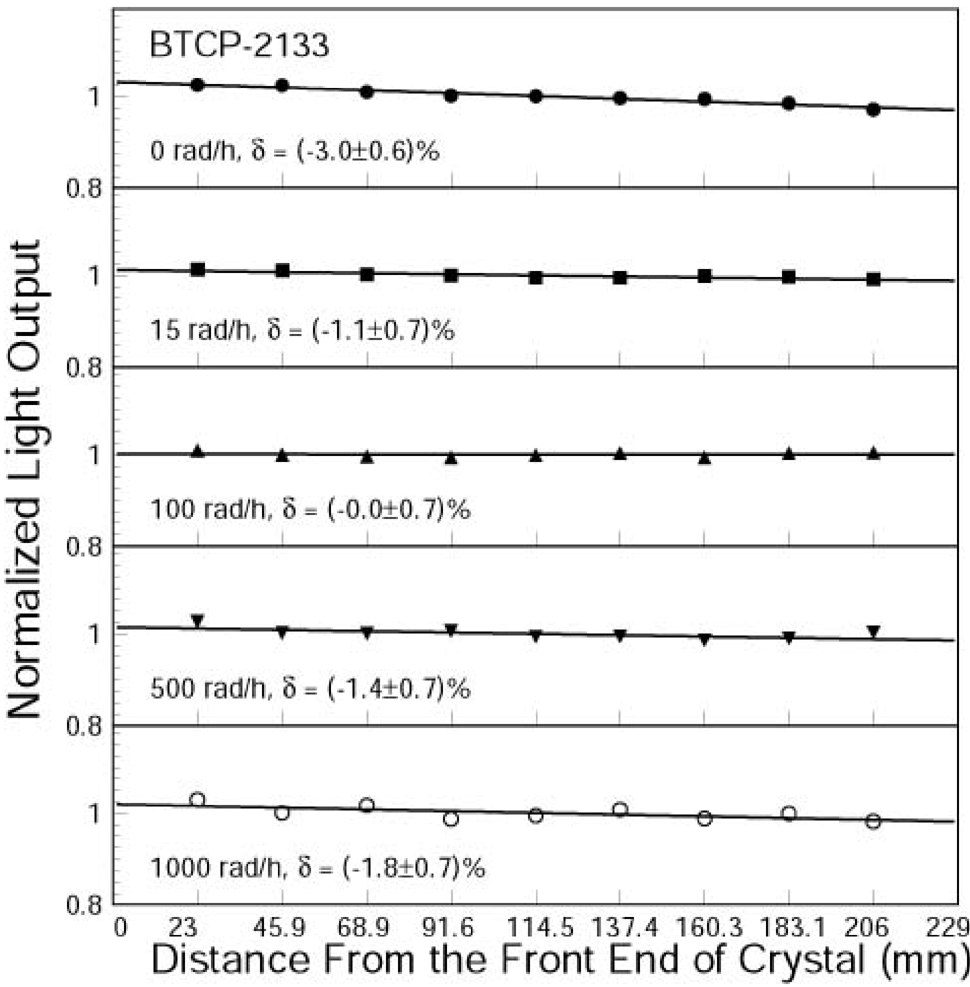

Dose Rate Dependence

IEEE Trans. Nucl. Sci., Vol. 44 (1997) 468-476

$$dD = \sum_{i=1}^{n} \{-a_i D_i dt + (D_i^{all} - D_i)\, b_i R dt\}$$

$$D = \sum_{i=1}^{n} \{\frac{b_i R D_i^{all}}{a_i + b_i R}[1 - e^{-(a_i + b_i R)t}] + D_i^0 e^{-(a_i + b_i R)t}\}$$

- D_i: color center density in units of m^{-1};
- D_i^0: initial color center density;
- D_i^{all} is the total density of trap related to the color center in the crystal;
- a_i: recovery costant in units of hr^{-1};
- b_i: damage contant in units of kRad^{-1};
- R: the radiation dose rate in units of kRad/hr.

$$D_{eq} = \sum_{i=1}^{n} \frac{b_i R D_i^{all}}{a_i + b_i R}$$

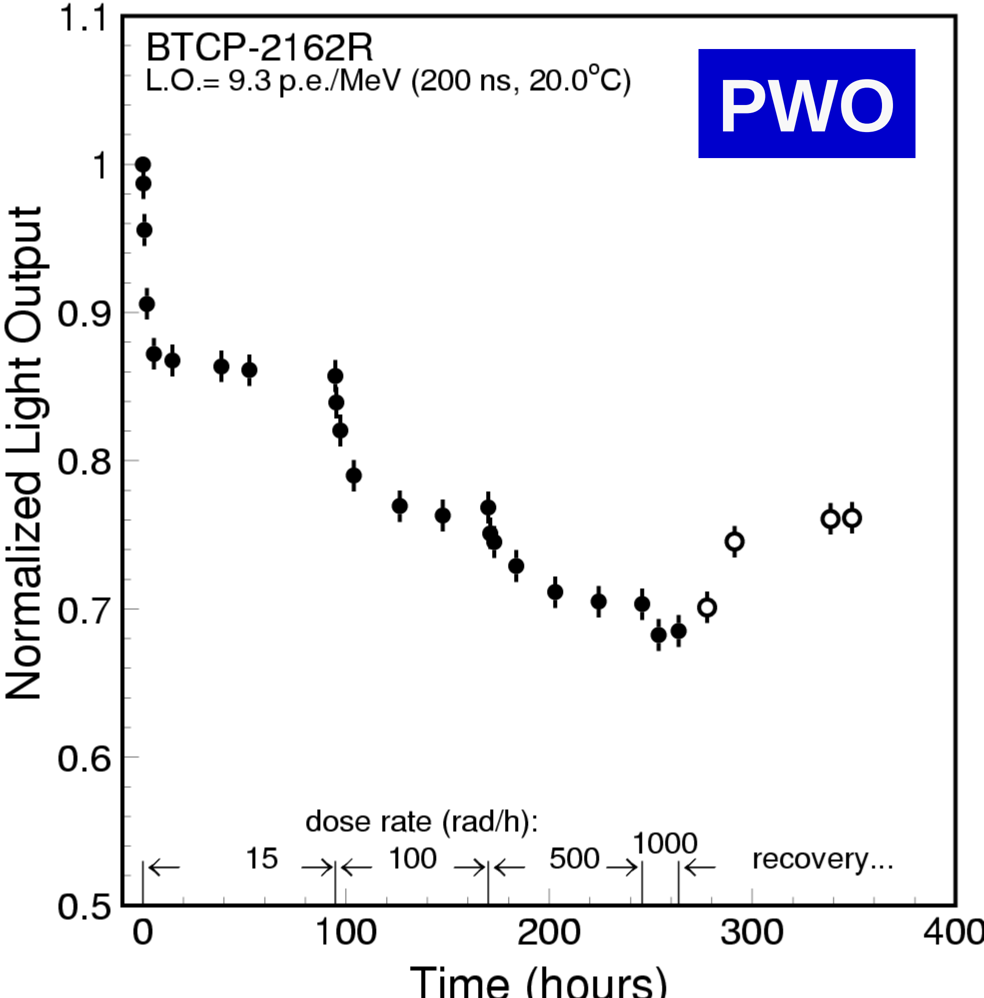

No Dose Rate Dependence

No/slow recovery: no/less dose rate dependence

BaF_2

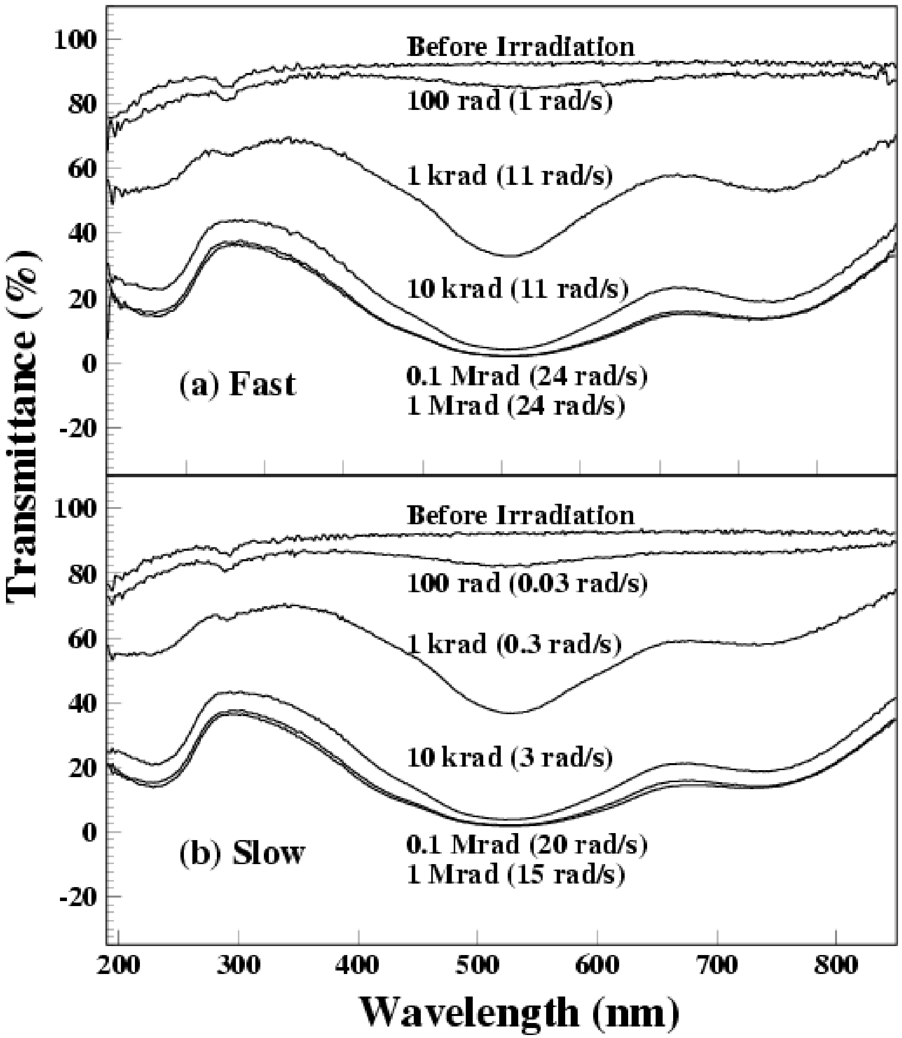

CsI(Tl)

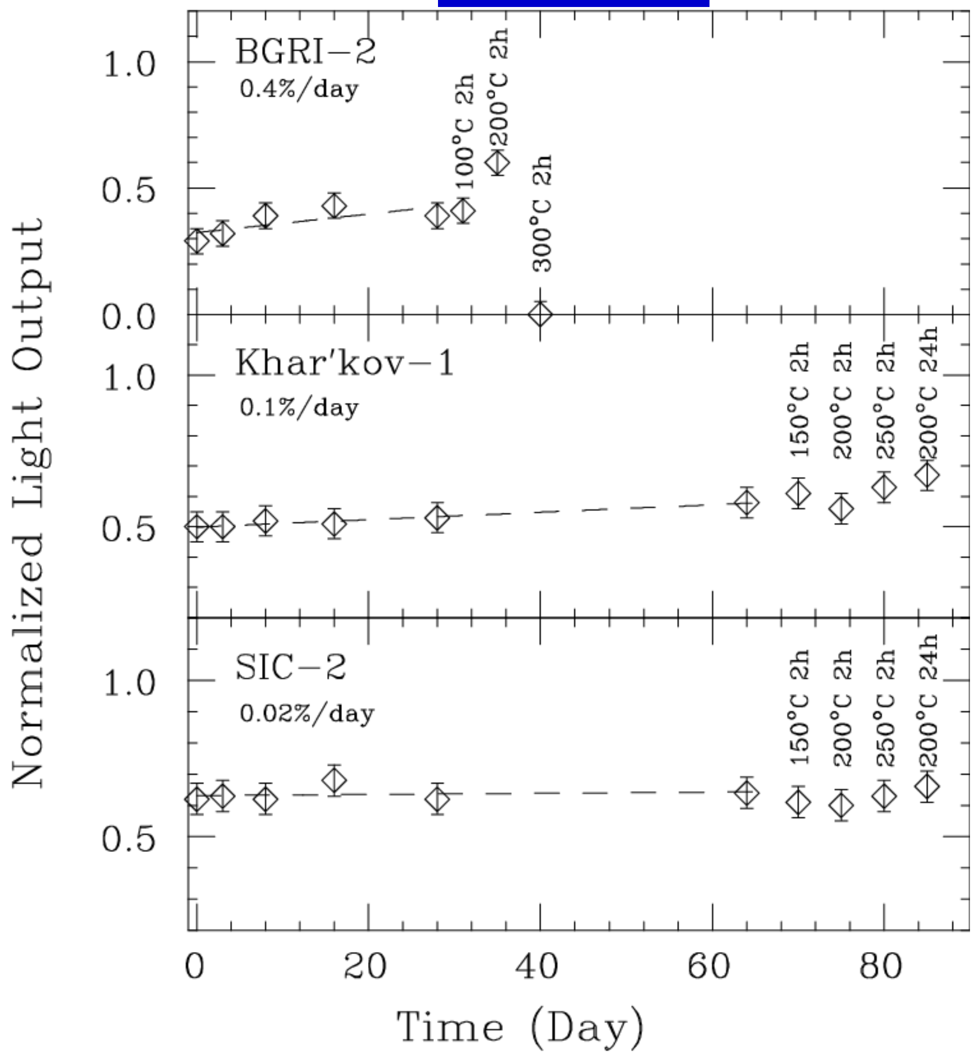

CsI(Tl) Damage Mechanism

Nucl. Instr. And Meth. A340 (1994) 442

- Oxygen Contamination is known to cause radiation damage for other alkali halide scintillators. In BaF_2, for example, hydroxyl (OH^-) may be introduced into crystal through a hydrolysis process, and latter decomposed to interstitial and substitutional centers by radiation through a radiolysis process: $H_i^0 + O_s^-$ or $H_s^- + O_i^0$, where subscript i and s refer to interstitial and substitutional centers respectively.
- Possible means for trace oxygen identification:
  - Secondary Ionization Mass Spectroscopy (SIMS);
  - Gas Fusion (LEGO); and
  - Energy Dispersive x-Ray (EDX).

PWO Radiation Damage Mechanism

Nucl. Instr. And Meth. A413 (1998) 297

- Crystal defects, such as Oxygen Vacancies, are known to cause radiation damage for other oxide scintillators. In BGO, for example, three common radiation induced absorption bands at 2.3, 3.0 and 3.8 eV were found in a series of 24 doped samples, indicating defect-related color centers.
- Possible means for oxygen vacancy identification:
  - Electron Paramagnetic Resonance (ESR) and Electron-Nuclear Double Resonance (ENDOR);
  - Transmission Electron Microscopy (TEM)/Energy Dispersion Spectrometry (EDS); and
  - A pragmatic way: Oxygen Compensation by Post-Growing Annealing in Oxygen Rich Atmosphere.

Mass Produced PWO Crystals

All samples: EWRIAC < 1 m^{-1} up to 400 rad/h
Rigorous QC required to qualify CMS endcap crystals

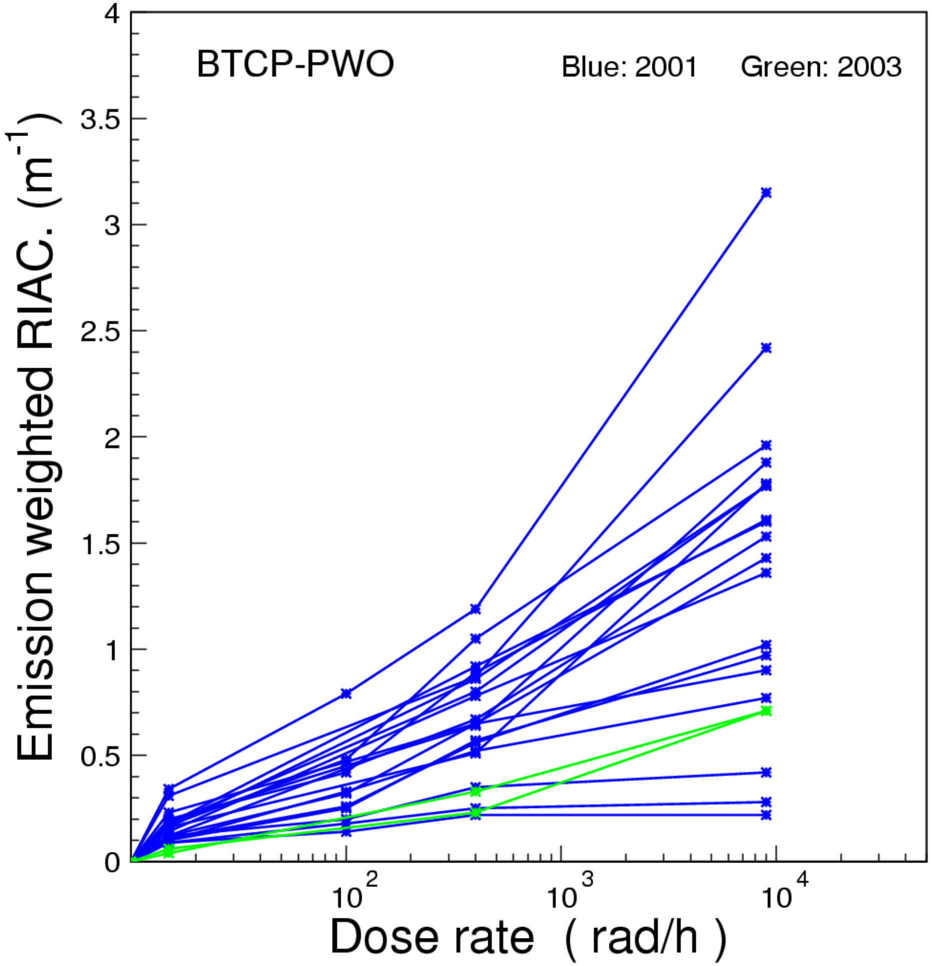

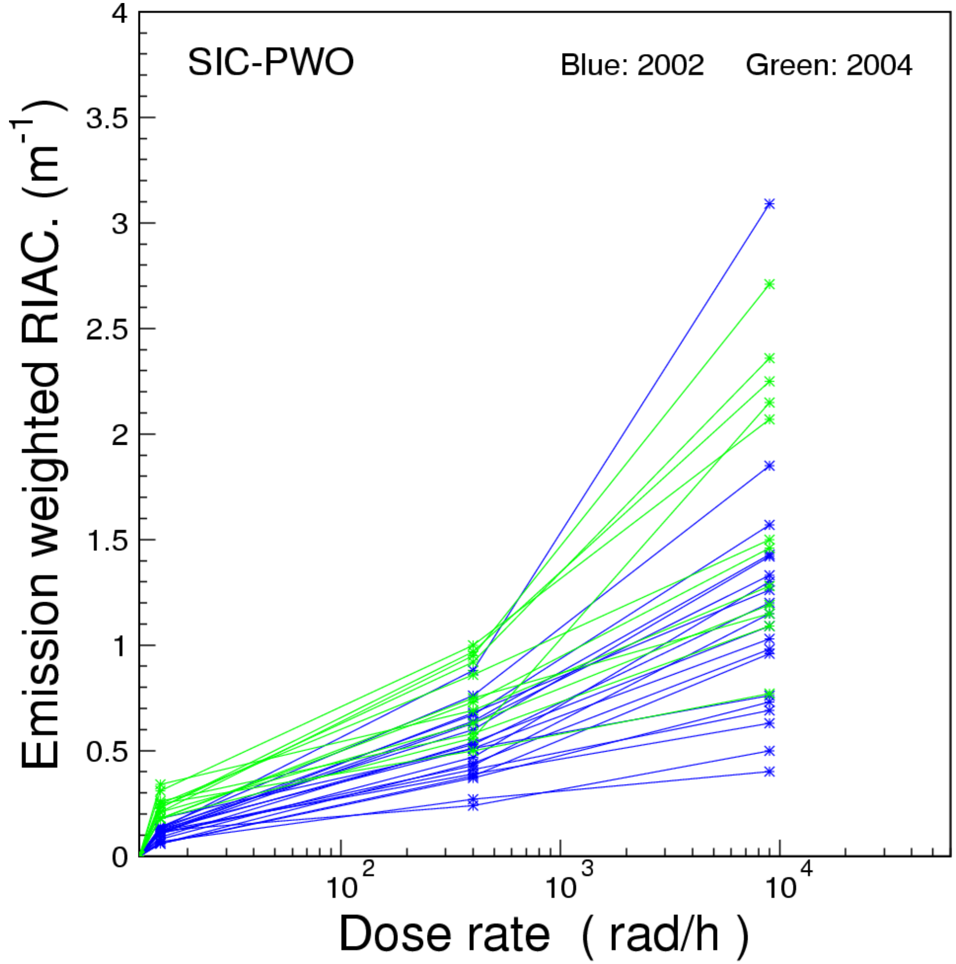

δLO/LO versus δLT/LT @ 100 rad/h

Strong correlation: Slope = 4.96

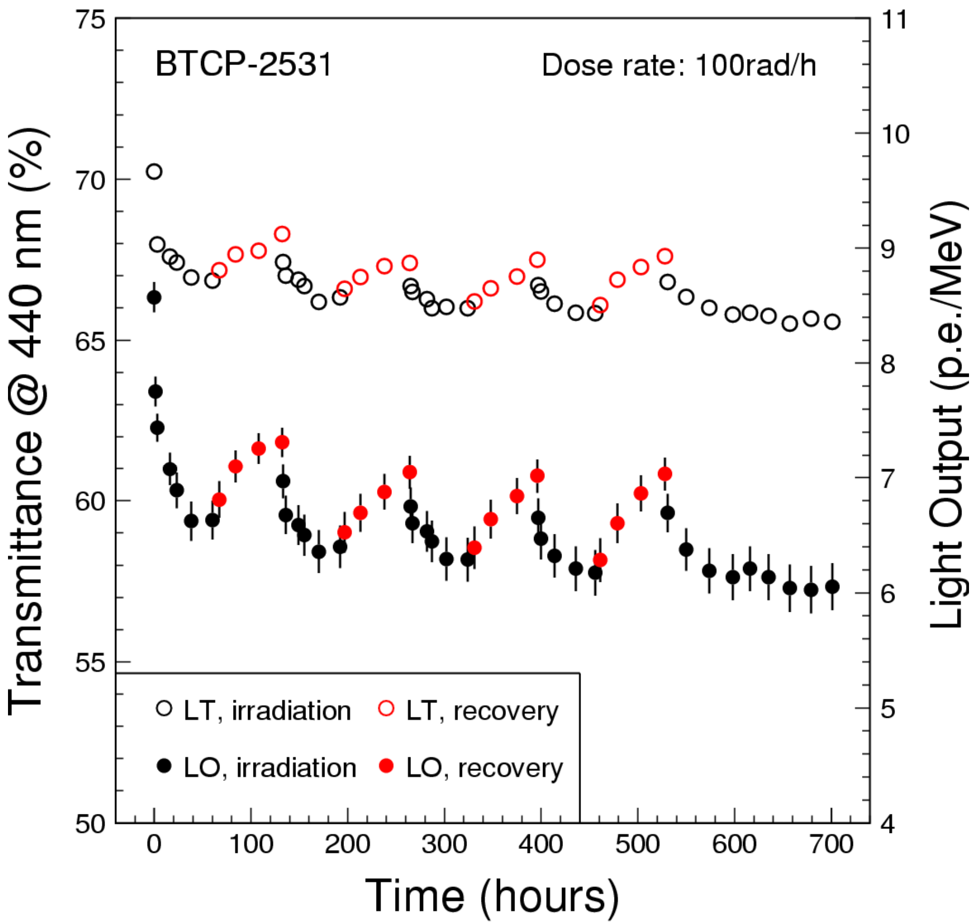

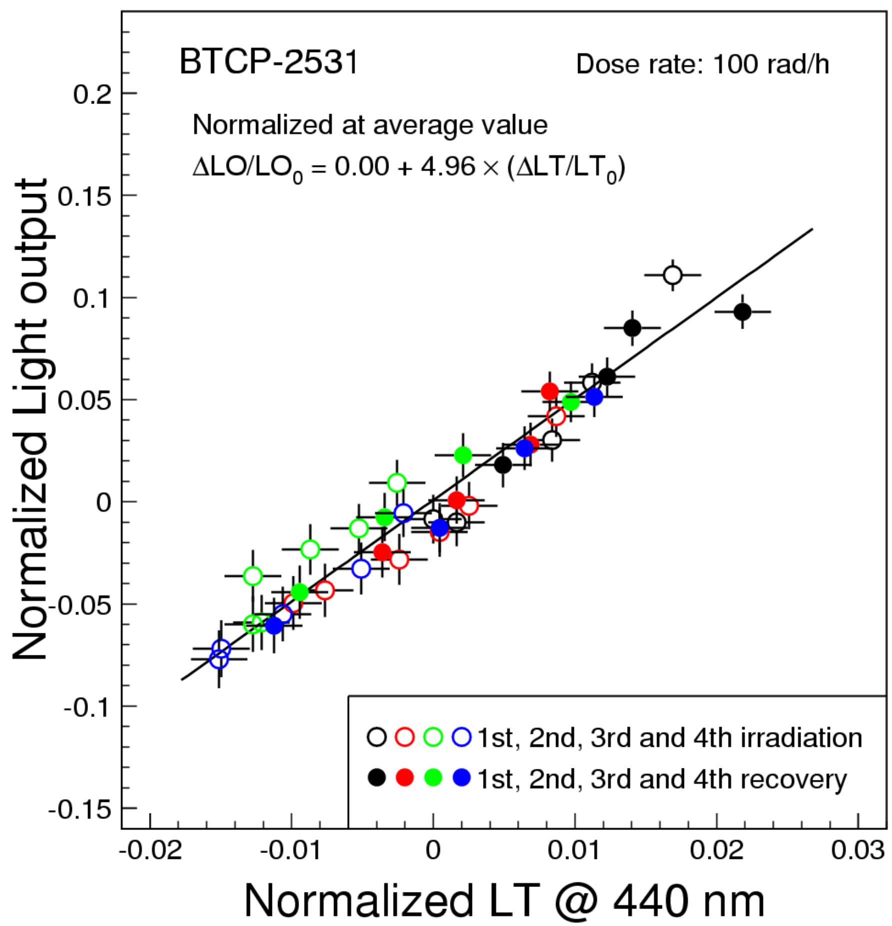

δLO/LO versus δLT/LT @ 100 rad/h

Strong correlation: Slope = 3.31

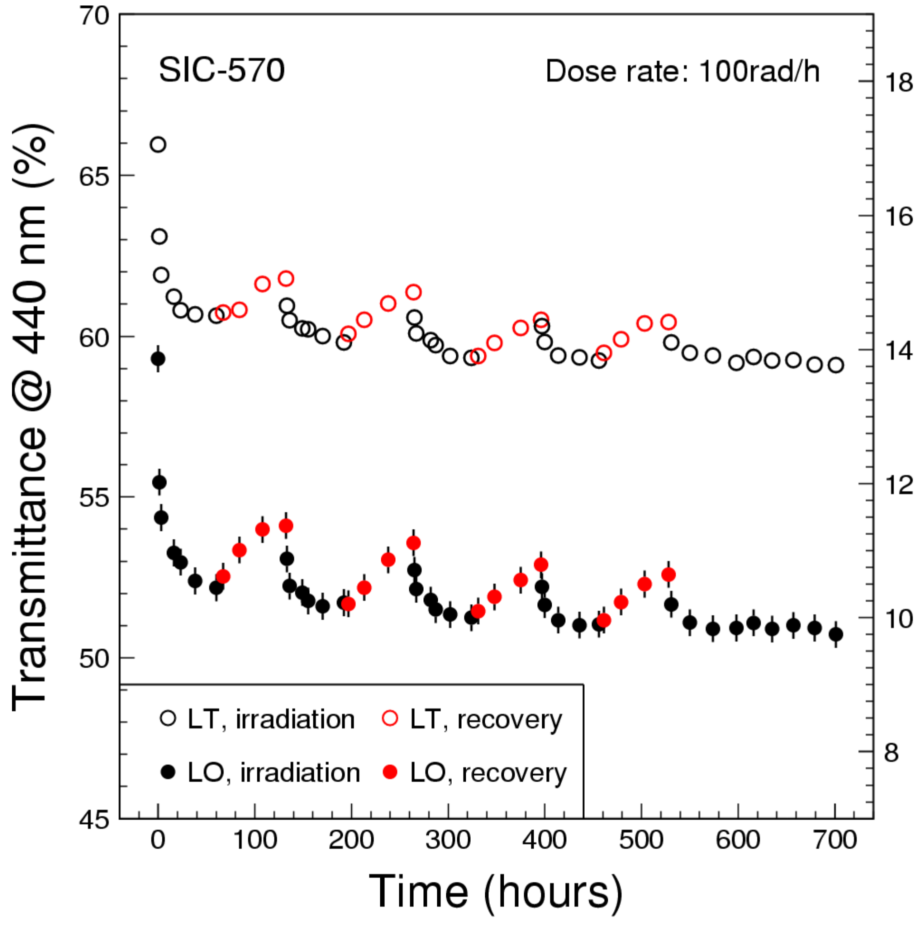

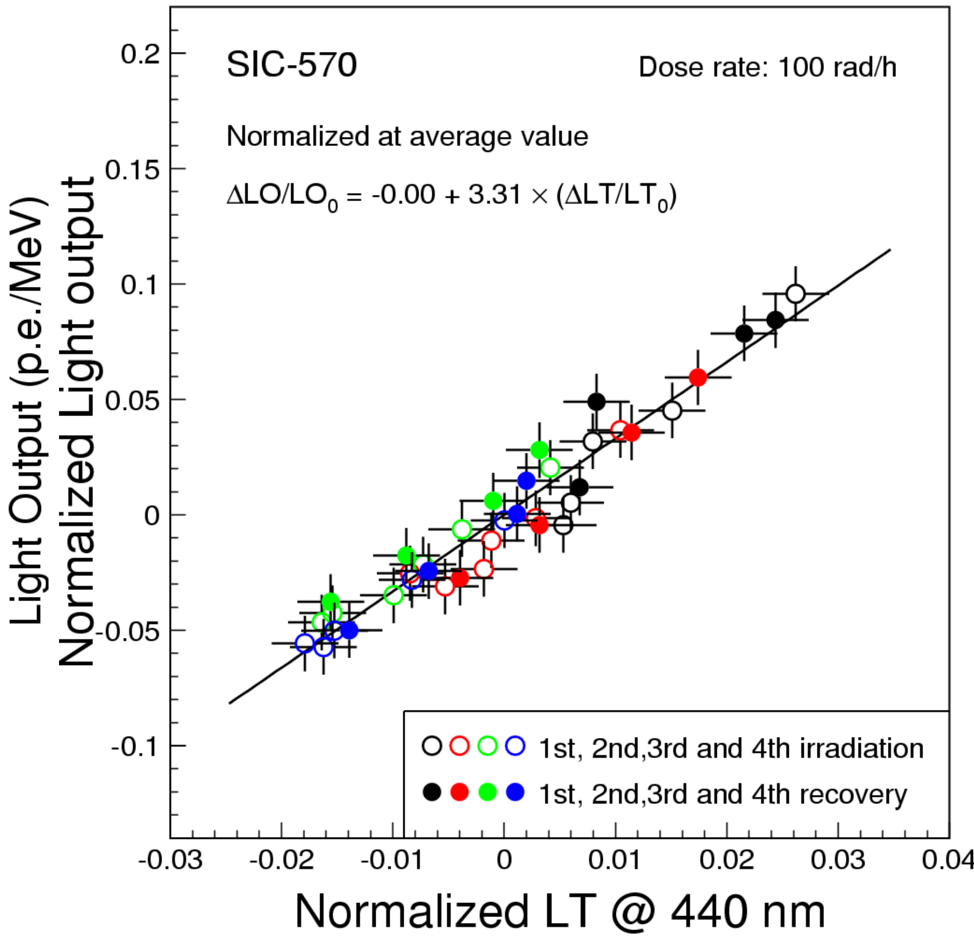

δLO/LO versus δLT/LT @ 400 rad/h

Strong correlation: Slope = 4.39

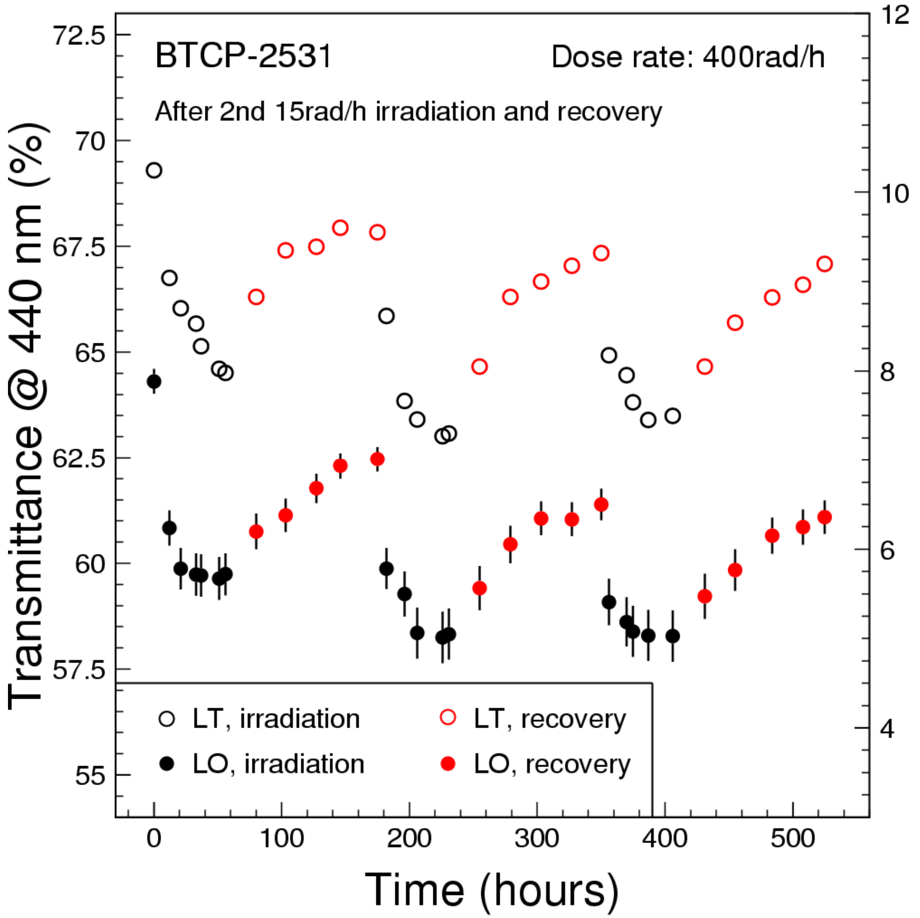

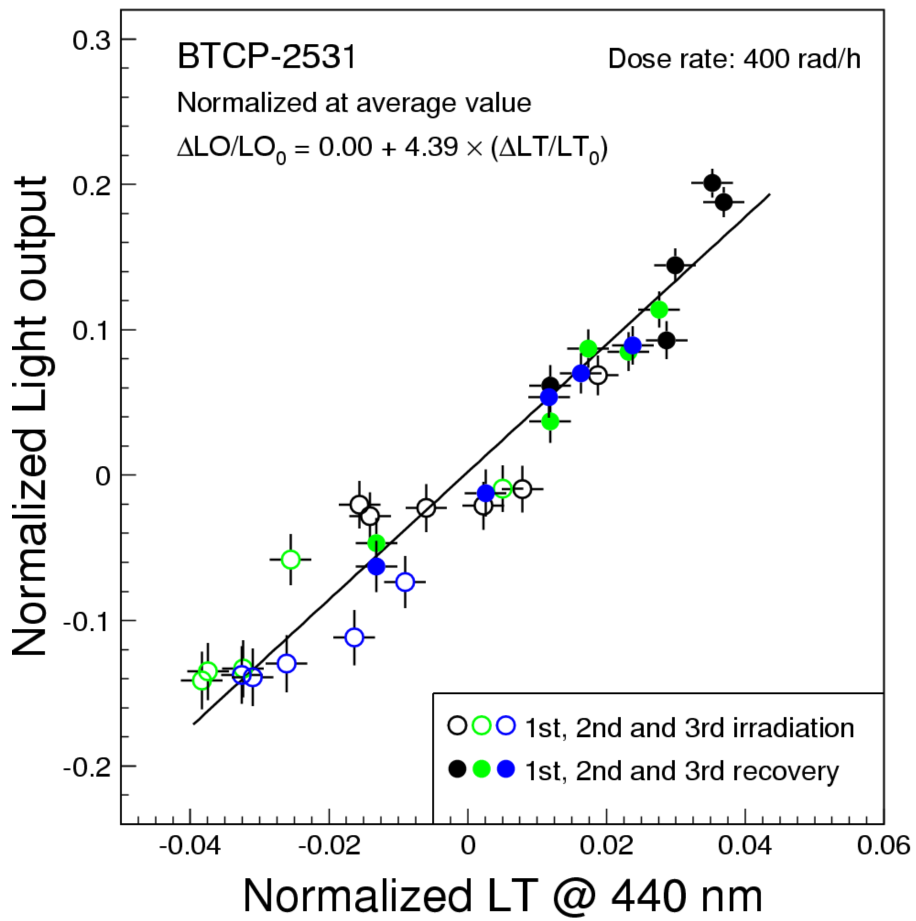

δLO/LO versus δLT/LT @ 400 rad/h

Strong correlation: Slope = 2.81

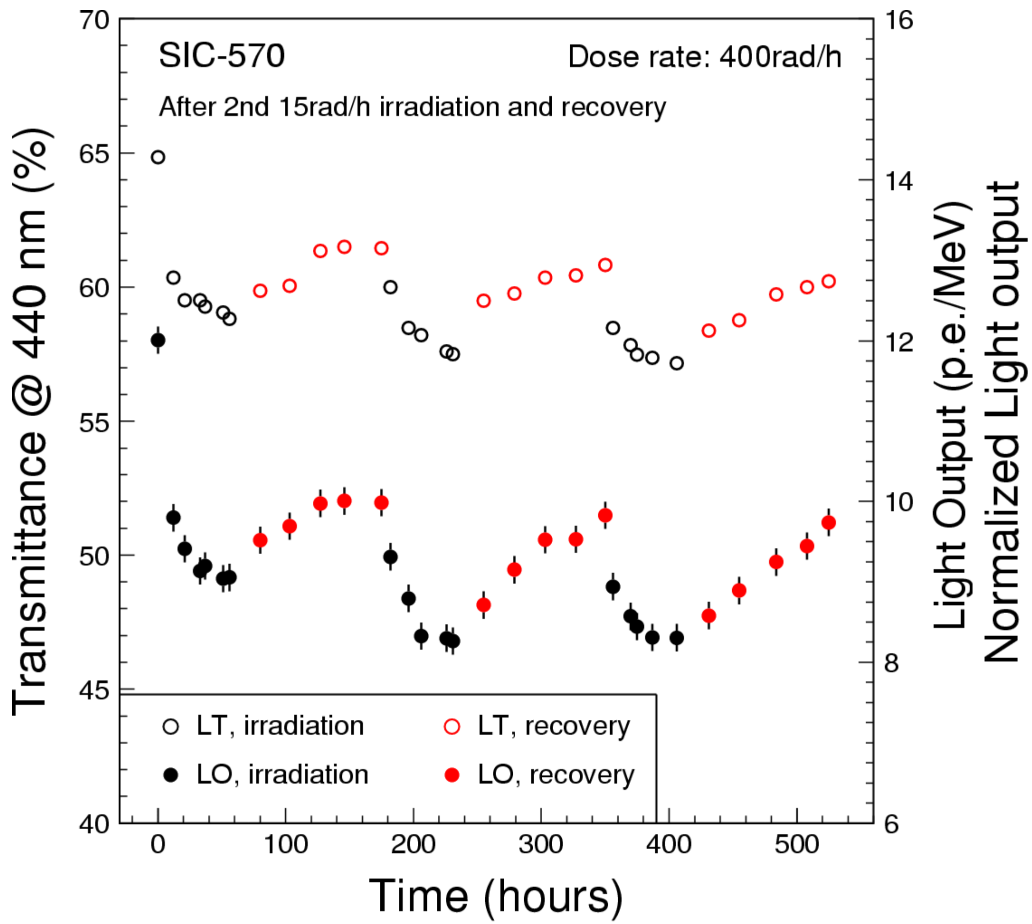

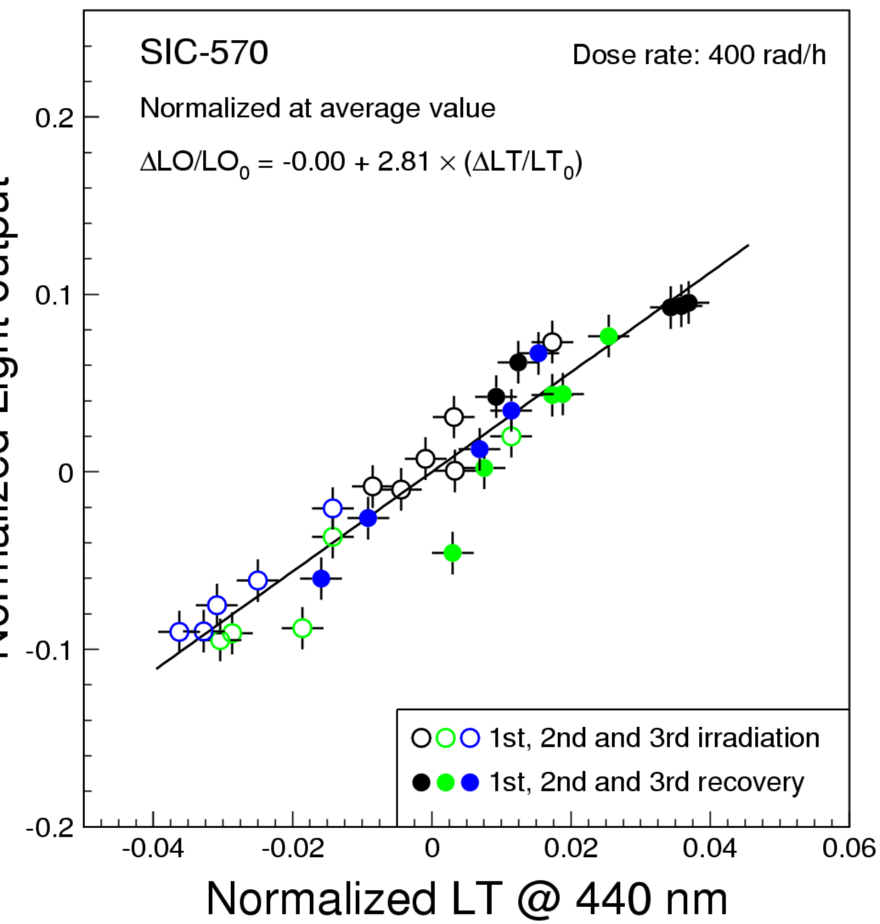

Radiation Induced Phosphorescence

Phosphorescence peaked at 430 nm with decay time constant of 2.5 h observed

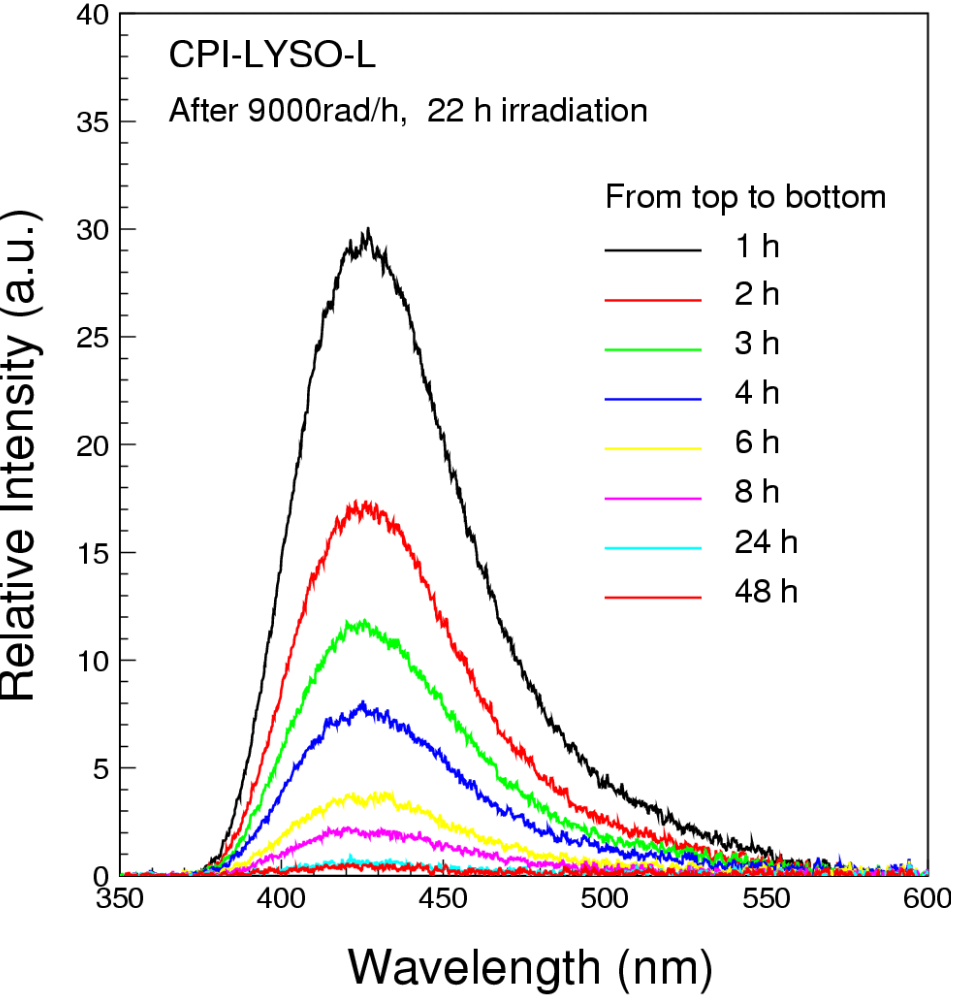

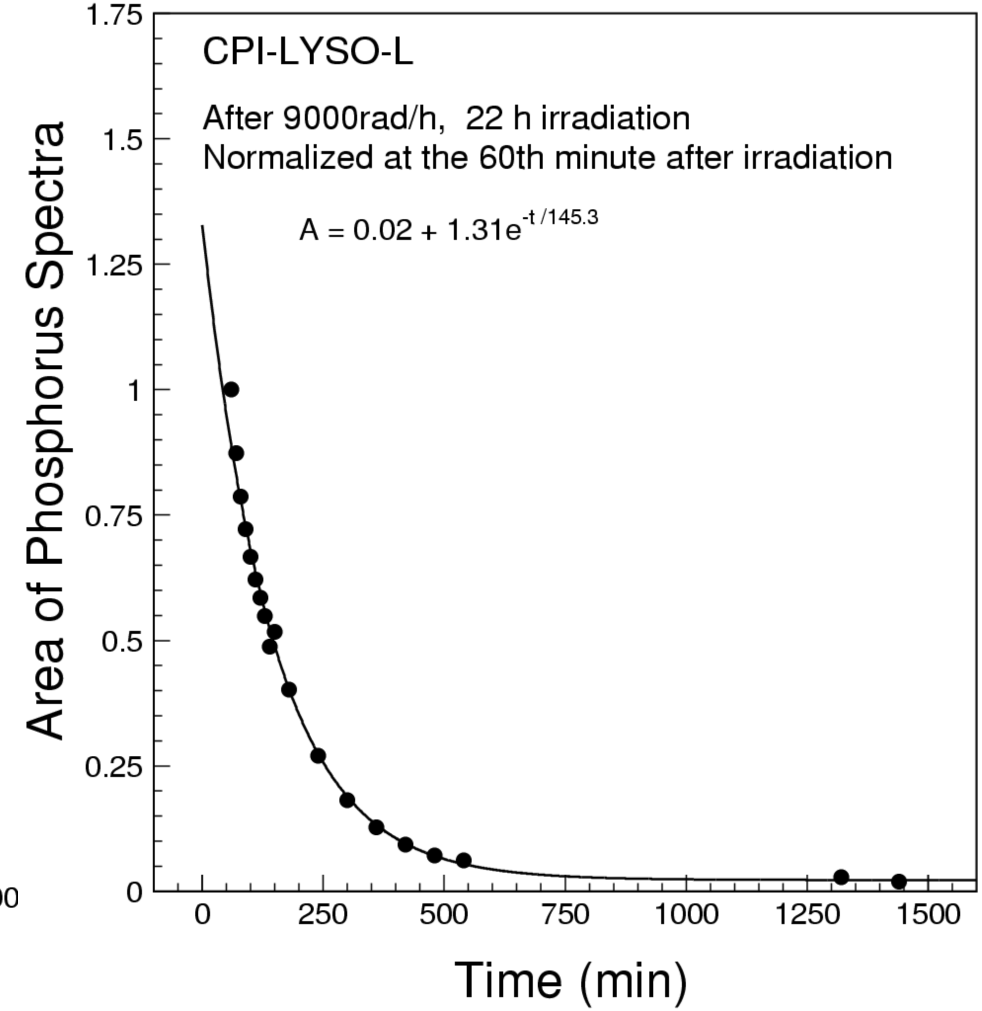

γ–ray Induced Readout Noise

Sample ID	L.Y. p.e./MeV	F μ A/rad/h	$Q_{15\ rad/h}$ p.e.	$Q_{500\ rad/h}$ p.e.	$\sigma_{15\ rad/h}$ MeV	$\sigma_{500\ rad/h}$ MeV
CPI	1,480	41	6.98×10^4	2.33×10^6	0.18	1.03
SG	1,580	42	7.15×10^4	2.38×10^6	0.17	0.97

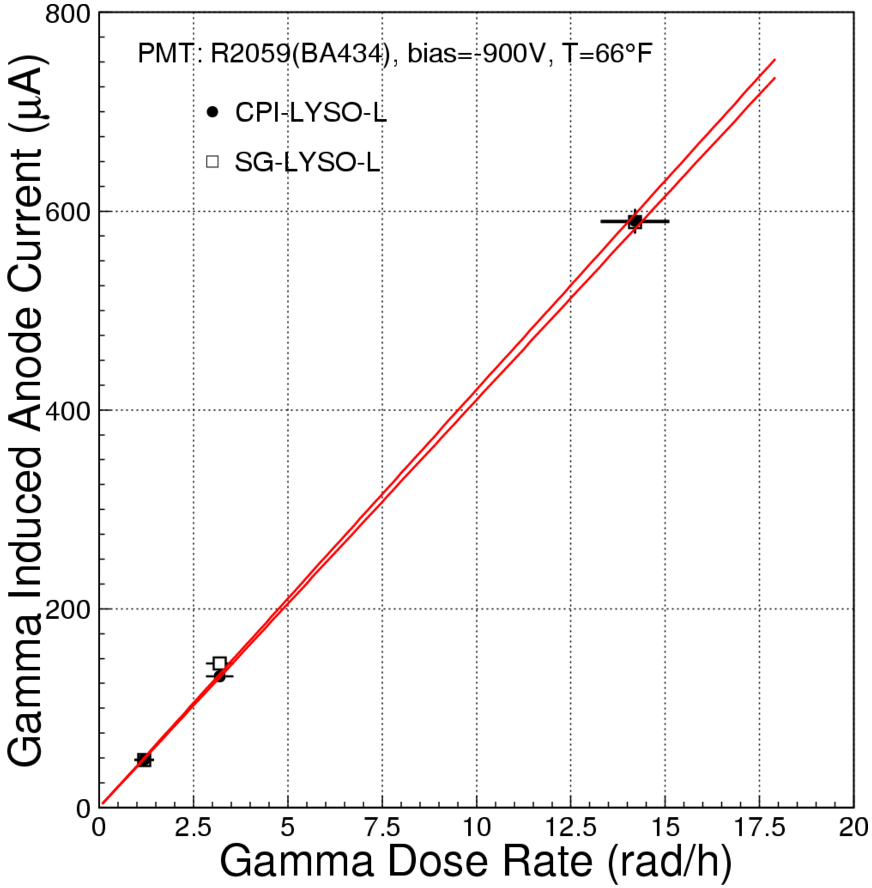

γ–ray induced PMT anode current can be converted to the photoelectron numbers (Q) integrated in 100 ns gate. Its statistical fluctuation contributes to the readout noise (σ).